ANNALS OF GEOPHYSICS, 56, 4, 2013, S0447; doi:10.4401/ag-6453

Special Issue: Vesuvius monitoring and knowledge

Groundwater geochemistry of the Mt. Vesuvius area: implications for volcano surveillance and relationship with hydrological and seismic signals

Cinzia Federico[1,*], Paolo Madonia[1], Paola Cusano[2], Simona Petrosino[2]

[1] *Istituto Nazionale di Geofisica e Vulcanologia, Sezione di Palermo, Palermo, Italy*

[2] *Istituto Nazionale di Geofisica e Vulcanologia, Sezione di Napoli, Osservatorio Vesuviano, Naples, Italy*

Article history
Received August 7, 2012; accepted December 17, 2012.
Subject classification:
Water chemistry, Seismicity, Hydrology, Volcanic surveillance.

ABSTRACT

Geochemical data obtained between 1998 and 2011 at the Mt. Vesuvius aquifer are discussed, focusing on the effects of both the hydrological regime and the temporal pattern of local seismicity. Water samples were collected in a permanent network of wells and springs located in the areas that are mostly affected by the ascent of magmatic volatiles, and their chemical composition and dissolved gas content were analyzed. As well as the geochemical parameters that describe the behavior of groundwater at Mt. Vesuvius, we discuss the temporal distribution of volcano-tectonic earthquakes. The seismological data set was collected by the stations forming the permanent and mobile network of the Istituto Nazionale di Geofisica e Vulcanologia - Osservatorio Vesuviano (INGV-OV). Our analysis of seismic data collected during 1998-2011 identified statistically significant variations in the seismicity rate, marked by phases of decreasing activity from October 1999 to May 2001 and increasing activity from August 2004 to mid-2006. The water chemistry shows peculiar patterns, characterized by a changeable input of CO_2-rich and saline water, which must be related to either a changing stress field or an increased input of CO_2-rich vapor. The water chemistry data from 1999 to 2003 account for both higher fluid pressure (which induced the seismic crisis of 1999 that peaked with a 3.6-magnitude earthquake in October 1999) and the increased input of CO_2-rich fluids. The highest emission of CO_2 from the crater fumaroles and the corresponding increase in dissolved carbon in groundwater characterize the phase of low seismicity. The termination of the phase of intense deep degassing is associated with a change in water chemistry and a peculiar seismic event that was recorded in July 2003. All these seismic and geochemical patterns are interpreted according to temporal variations in the regional and local stress field.

Introduction

Fluids circulating in volcanic edifices are attracting increasing interest from scientists, mostly because their role in triggering flank instability, phreatic explosions, and eruptions has been documented in dozens of cases worldwide [Day 1996, Reid 2004, Thomas et al. 2004]. Internal pressurization of magmatic volatiles and hydrothermal systems can lead to dramatic steam blasts and, eventually, to eruptions [Hill et al. 2002]. The fluid pore pressure can also be changed by external mechanisms, such as variation of the stress field or, more generally, variation of the porosity/permeability of volcanic rocks. Static or dynamic stress changes, which have a clear expression in seismicity, exert a significant control on fluid patterns and eventually on the ascent of melts [Newhall et al. 2001, Hill et al. 2002, Mortimer et al. 2011]. The reciprocal roles of tectonics and magmatic/hydrothermal activity, and their influence in determining the so-called crises, is still under investigation [Roeloffs et al. 2003, Gottsman et al. 2007]. Monitoring of groundwater in volcanic systems is useful for predicting changes in the tectonic and volcanic stress field [Newhall et al. 2001, Hurwitz and Johnston 2003, Biagi et al. 2004, Koizumi et al. 2004]. Changes in water level in some wells were observed prior to the 2000 eruption of Mt. Usu, Japan [Shibata and Akita 2001], and is a frequent characteristic in eruptions of Mt. Vesuvius [Bertagnini et al. 2006].

Mt. Vesuvius hosts a shallow aquifer which receives magmatic/hydrothermal gases mostly in correspondence of the main tectonic lineaments [Federico et al. 2002]. Some changes in water and dissolved gas composition have been recorded in concomitance with the seismic crisis that occurred in 1999 [Federico et al. 2004, Madonia et al. 2008].

The present study aimed at elucidating the roles of both the stress field and the magmatic/hydrothermal degassing in changes in water chemistry in the vesuvian shallow aquifer. We report on the composition of major ions, temperature, and dissolved gas con-

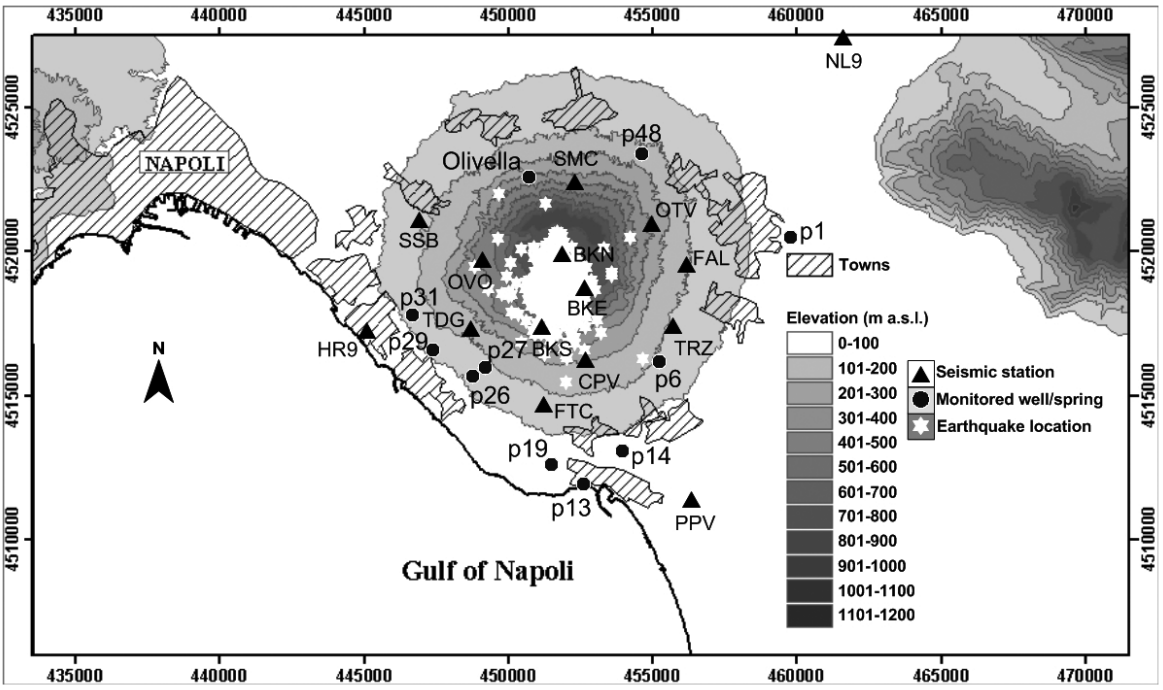

Figure 1. Map of the Mt. Vesuvius area showing the locations of earthquakes and measuring points of the seismic and geochemical surveillance networks.

tents (which were partly reported by Madonia et al. [2008]) measured between 1998 and 2011 at selected springs and wells located on the lower flanks of Mt. Vesuvius. Temporal variations of water chemistry can be attributed to either changes in porosity/permeability and fluid circulation or the input of CO_2-rich vapor, and provide insights into the present rest period. Finally, we compare the variations of the geochemical parameters with those of the seismic activity.

Study area

Geological summary

With a radius of ca 10 km, the Somma-Vesuvius complex (1281 m a.s.l.) in southern Italy is a polygenetic volcanic complex composed of an old stratovolcano (Somma), which is mainly preserved on the northern sector of the edifice, and the younger cone of Mt. Vesuvius (Figure 1). The Somma-Vesuvius complex developed within a wide gravimetric anomaly located in the central part of the Campanian Plain (a depression bordered by Tertiary and Mesozoic carbonate massifs) named the Acerra graben [Scandone et al. 1991, Marzocchi et al. 1993]. This anomaly is related to the subsidence of the carbonate basement lying about 2 km beneath Mt. Vesuvius. The stratovolcano developed at the intersection of two regional tectonic fault systems (running NW–SE/NNW–SSE and NNE–SSW/NE–SW). In addition to these two regional structures there are also local eruptive fractures aligned in the E–W and N–S directions inside the Somma caldera and on the southern flank of the volcano [Bianco et al. 1998].

The volcanic activity of the volcanic complex has been characterized by the alternation between pyroclastic eruptions (separated by quiescent periods) and open conduit phases, characterized by Strombolian and effusive activity [Santacroce et al. 1994, Cioni et al. 1998]. The Somma volcano mainly consists of lava flows (K-rich basalts and latites) and minor pyroclastics (strombolian scoria fall deposits) and was active between 25 and 18 ka BP [Santacroce 1987, Ayuso et al. 1998]. Four Plinian eruptions between 18 ka BP and A.D. 79 caused the summit to collapse and gave rise to the formation of a multistage summit caldera (i.e., the Somma caldera) [Santacroce 1987, Andronico et al. 1995, Principe et al. 1999, De Vivo and Rolandi 2001]. After the sub-Plinian eruption in 1631, an open conduit phase lasted until the 1944 eruption, since when the volcano has been in a state of weak volcanic-hydrothermal activity characterized by diffuse CO_2 degassing and low-temperature fumarolic activity in the crater area, thermal submarine features, and low seismic activity [Aiuppa et al. 2004, Del Pezzo et al. 2004, Frondini et al. 2004, Caliro et al. 2011].

Seismicity

The natural vesuvian seismicity mainly consists of volcano tectonic (VT) earthquakes [Chouet 1996], which are characterized by clear P- and S-wave packets and a high-frequency content, mostly peaking in the band 5-15 Hz. They are usually located within a volume centered along the crater axis, at depths shallower than

about 4 km below sea level (b.s.l.). The transition zone between the volcanic edifice and the carbonate basement, at 2-3 km b.s.l., coincides with the maximum of the spatial distribution of the hypocenters [Saccorotti et al. 2002, Scarpa et al. 2002, Del Pezzo et al. 2004].

Assumptions about the source dynamics for the vesuvian VT earthquakes involve failures in the brittle rocks, with strike-slip and normal/reverse dip-slip focal mechanisms. A wide variety of nodal plane orientations is indicated, but overall the directions are NW–SE and NE–SW [Bianco et al. 1998, Ventura and Vilardo 1999]. The P and T axes are mainly assumed to be present along the NNE–SSW and ESE–WNW directions and along the ESE–WNW and NNE/N–SSW/S directions, respectively [Bianco et al. 1998, Ventura and Vilardo 1999, Zollo et al. 2002].

According to Del Pezzo et al. [2004], the deepest events are associated with average stress drop between 1 and 10 MPa and are mainly caused by the release of regional tectonic stress in the prefractured carbonate basement. On the other end, the shallowest earthquakes are characterized by stress drop of up to 1 MPa and are probably triggered by increasing pore fluid pressure caused by changes in the hydrothermal aquifer, which is located beneath the crater at about 1 km b.s.l.

Madonia et al. [2008] revealed two statistically significant variations in the seismicity behavior between 1998 and 2005: in May 2001 and July 2004. Two phases corresponding to these variations can be identified. The first is relative to the 1999 crisis. The highest-magnitude (3.6) earthquake since the last eruption (in 1944) occurred during this crisis, at 07:41 UT on October 9, 1999. This earthquake was located about 4 km beneath the crater area, inside the carbonate basement. Several studies have demonstrated that this event was generated by tectonic stress release along a pre-existing fracture system [Ventura and Vilardo 1999, Zollo et al. 2002, Del Pezzo et al. 2004]. This was followed by a sequence of low-energy earthquakes, and the seismic activity decreased up to May 2001. Low levels of seismicity were observed until July 2004, when a slight increase in the seismicity rate marked the beginning of the second phase.

Hydrogeology

Two main aquifers exist in the vesuvian area [Corniello et al. 1990, Celico et al. 1998]: (1) a deep carbonate aquifer hosted in the buried Mesozoic series beneath the Campanian Plain and recharged by precipitation falling on the Apennines, and (2) a shallower volcanic aquifer (the vesuvian aquifer) hosted in fractured lavas and coarse-grained pyroclastic deposits of the Somma-Vesuvius complex. As generally observed in stratovolcanoes, water at Mt. Vesuvius circulates in several overlapping water bodies separated by impermeable fine-grained pyroclastic layers. The transmissivity values of these aquifers range from 10^{-4} to 10^{-1} $m^2 \cdot s^{-1}$ [Celico et al. 1998], with the highest values (10^{-2} to 10^{-1} $m^2 \cdot s^{-1}$) being found on the southern flank of the volcano. The exchanges between the deep and shallow water bodies are easier in this area due to both the volcanic cover being thinner and the presence of fractures in the carbonate basement, which facilitate upward water circulation.

The numerous studies concerning the chemistry of Somma-Vesuvius groundwaters have clarified the mechanisms of gas–water–rock interactions, highlighting the role of volcanic CO_2 in controlling rock leaching and water chemistry [Caliro et al. 1998, Celico et al. 1998, Federico et al. 2002, Aiuppa et al. 2005, Caliro et al. 2005]. Analysis of stable isotopes in dissolved gases (CO_2 and He) have demonstrated that magmatic volatiles are actively transported by groundwaters flowing along the main faults and fractures, trending NW–SE and NE–SW, which affect both the volcanic edifice and the sedimentary basement [Federico et al. 2002]. Moreover, a systematic contrast in the chemical compositions of the groundwaters flowing on the southern and northern sectors of the volcanic edifice has been demonstrated, with the former being typically characterized by higher outlet temperatures, total dissolved solids, and dissolved CO_2 contents. These findings clearly indicate that the gas supply is lower on the northern sector of the volcano than on the southern one, which could be ascribed to a structural-geological control of water circulation. According to Federico et al. [2002], carbonate groundwaters flowing from the Apennines to the Tyrrhenian Sea would interact with the central conduit system, thus becoming heated and gas-charged by the ascending hot fluids sustained by deep magma degassing. Further south these CO_2-charged carbonate groundwaters may represent a CO_2 source for the shallow volcanic aquifer, for example in the Torre Annunziata area, where the carbonate aquifer lies at a depth of only 500 m [Celico et al. 1998]. In an alternative proposed model the northern walls of the Somma caldera represent an impermeable barrier to water infiltration, thus forcing groundwaters to flow southward [Federico et al. 2002, Caliro et al. 2005], in which case the groundwaters would dissolve CO_2 mainly in the crater area [Caliro et al. 2005].

Methods

The seismological monitoring of Mt. Vesuvius is performed by INGV-OV personnel using a permanent seismic network that has been active since 1972. Currently the monitoring network consists of 10 stations

equipped with short-period geophones, of which 3 are three-component stations and 2 are short-period three-component digital stations. Moreover, six broadband three-component digital stations are present in the crater area. The installed sensors are 1-Hz velocimeters (Geotech S13 and Mark LE-3D) and broadband sensors (Guralp CMG 40T and Trillium 120P). Seismic data are continuously acquired at 100 sample·s^{-1}, transmitted to an acquisition center in Naples, and stored on hard disks. More information is available in Giudicepietro et al. [2010].

The Mobile Seismic Network of INGV-OV has installed four digital stations at Mt. Vesuvius. MARSlite and Lennartz M24 devices equipped with three-component broadband sensors (Guralp CMG-40T or Lennartz LE-3D/20s) operate on the volcano. The signals are acquired in situ at a sampling rate of 125 or 100 Hz. Further technical details are available elsewhere [Castellano et al. 2012].

A seismic catalogue of Mt. Vesuvius, which contains the occurrence time and the duration magnitude (M_D) values of the VT earthquakes, has been compiled since 1972. The relation between the magnitude and the seismic trace duration was calibrated by Del Pezzo et al. [1983] for vesuvian VT earthquakes recorded on the vertical component of the OVO station, located in the western sector of the volcano (Figure 1). Figure 2 shows the monthly distribution of the number of VT earthquakes based on this catalogue. The vesuvian VT earthquakes included in the catalogue were localized using a 3D probabilistic algorithm (NonLinLoc) [Lomax et al. 2000] over the 3D velocity model inferred by Scarpa et al. [2002]. The hypocenter depth as a function of the time is reported in Figure 2.

The hydrogeochemical parameters of the vesuvian aquifer have been monitored since 1998. The first hydrogeochemical monitoring network consisted of 10 private wells that were mainly used for irrigation and 2 springs (Figure 1). Currently the network consists of six

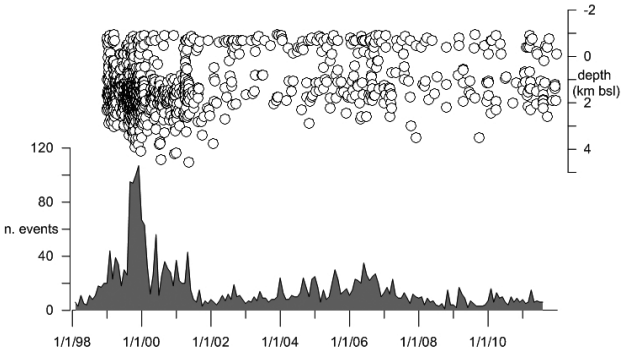

Figure 2. Hypocentral depths of vesuvian VT earthquakes as functions of time (upper panel) and the monthly number of VT earthquakes (lower panel).

wells and two springs, while temperature is recorded hourly at selected sites (data not shown). Temperature, pH, Eh, and alkalinity were determined by sampling with conventional field instrumentation; laboratory determinations were carried out at INGV, Palermo, following the procedures described by Federico et al. [2002]. The concentrations of major ions were measured by applying ion chromatography to filtered (Cl^-, NO_3^-, and SO_4^{2-}) and filtered and acidified (Na^+, K^+, Ca^{2+}, and Mg^{2+}) samples, with an analytical uncertainty of <5%. The dissolved gases in water samples were measured after equilibration in a host gas (Ar) and extraction, following the procedure described by Capasso and Inguaggiato [1998]. Analyses were performed using a gas chromatograph (Perkin-Elmer 8500), equipped with 4-m Carbosieve II columns and two detectors (hot wire and flame ionization), with Ar as the carrier gas. The analytical uncertainty was <5%.

Results

The number of VT earthquakes peaked at the time of the October 1999 seismic crisis. The earthquakes belonging to this crisis occurred in the prefractured carbonate basement in response to a release of the regional tectonic stress and are characterized by deep locations and large reductions in stress drop values [Del Pezzo et al. 2004]. The effects of this crisis lasted until the beginning of 2002, after which the seismic activity decreased to very low levels. The hypocenters clustered within the volcanic edifice at depths in the range 0-2.5 km diminished dramatically, and those deeper than 2.5 km practically disappeared. Moreover the stress drop assumed low values. As asserted by many authors [Saccorotti et al. 2002, Del Pezzo et al. 2004], it is likely that most of these VT earthquakes were caused by variations of the pore fluid pressure. These variations could be induced by the local stress perturbations themselves or by charging and discharging mechanisms of the shallow aquifer.

On July 20, 2003, an anomalous low-frequency earthquake with a quasimonochromatic spectrum in the frequency band of 3.5-4 Hz was recorded by all of the stations of the INGV-OV seismic network. It was located at about 4 km b.s.l., and Bianco et al. [2005] reported that it was probably of hydrothermal-volcanic origin.

A slight seismic anomaly began in August 2004, after which the number of VT earthquakes began to increase, reaching a relative maximum in 2006 before returning to very low values. This period included an earthquake (on August 30, 2005) at the very shallow depth of 300 m a.s.l. Using a combination of seismological and geochemical methods, Madonia et al. [2008]

modeled the source mechanism of this VT earthquake as the superposition of tensile cracking and shear failures. The crack opened along the direction orthogonal to the maximum stress axis of the faulting, due to an increase of the pore fluid pressure. This increase could in turn be caused by the variation of the local stress field that enhanced the upward migration of thermal fluids. The 2005 year was also characterized by the absolute minimum of deep seismicity.

As shown by Federico et al. [2002, 2004], the waters circulating through the vesuvian aquifers are characterized by large spatial and temporal variations in chemical composition (Figure 3). In general, these waters are rich in HCO_3^- and their alkali content (here represented by the K^+ content) is strictly controlled by the CO_2-driven mechanism of rock dissolution. Nevertheless, a variable enrichment in either Cl^- or SO_4^{2-} with respect to the volcanic rock is observed. Sample 14 shows the lowest relative content of SO_4^{2-}, while its relative content of Cl^- is higher than that in the host rock.

As suggested by Federico et al. [2002], the southern sector of the vesuvian aquifer is characterized by the local ascent of brine-type warm fluids along faults. Among collected samples, well 14 is the most saline ($Cl = 2000\ mg \cdot l^{-1}$ on average) and, together with spring 13, it is the warmest, which suggests that it is contaminated by hot Cl-rich brines.

The enrichment in SO_4^{2-}, which is mostly observed in samples (namely sites 13, 19, and 29) collected in the Torre Annunziata–Torre del Greco area (where S-rich gas manifestations have been identified along the coast), can be attributed to either the oxidation of hydrothermal S-bearing minerals (i.e., pyrite) or the dissolution of a H_2S-bearing gas phase by groundwater during circulation at depth [Federico et al. 2002]. The enrichment of SO_4^{2-} in a few of the wells can be ascribed to the contribution of fluids related to human activities, in particular to the use of SO and N-rich fertilizers or rural sewage, as suggested by Federico et al. [2004]. This effect is evident in samples 47 and 19, which also have higher NO_3^- contents (see Appendix).

During the monitored period the vesuvian groundwater exhibited compositional variability, which can be quantified as SO_4^{2-}/HCO_3^- and Cl^-/SO_4^{2-} ratios (Figure 3a). Moreover, significant changes in water salinity are observed at some sites. Figures 4-7 plot the time trends of some significant parameters at selected sites during the entire monitored period.

Figure 4 displays the time trends of the water temperature measured at sites 13, 14 and 29. A common feature is the small (<1°C) and slow increase in temperature after the 1999 earthquake, with a marked decrease of as high as 4°C occurring after 2003 or 2006 (spring 13).

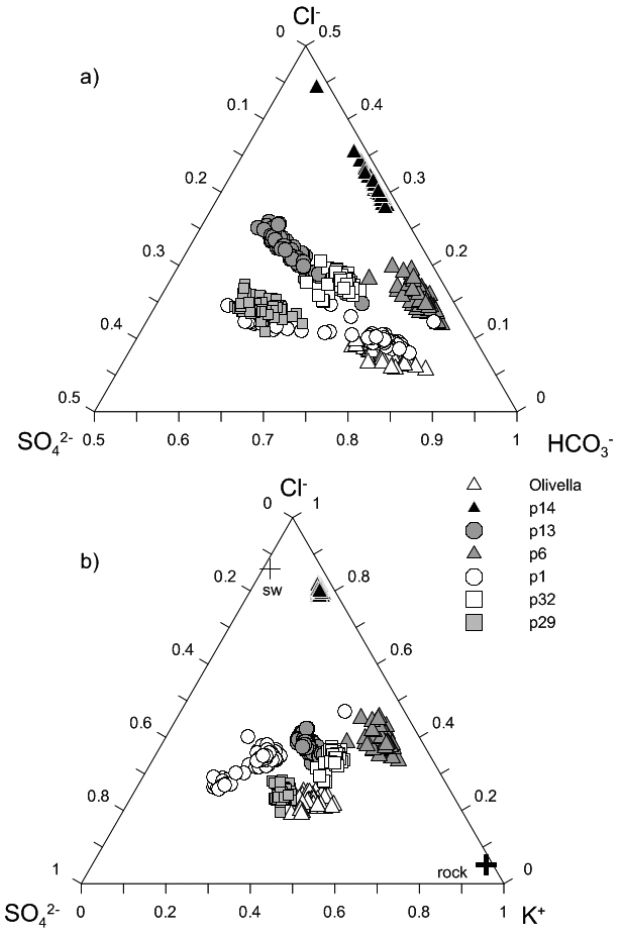

Figure 3. a) Cl^--SO_4^{2-}-HCO_3^- triangular diagram. b) Cl^--SO_4^{2-}-K^+ triangular diagram. The average composition of lava and scorias from Belkin et al. [1998] and the point representative of seawater are plotted for comparison. Concentrations are expressed in units of $mg \cdot l^{-1}$.

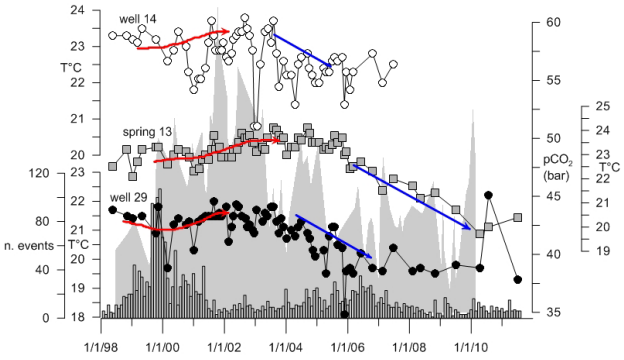

Figure 4. Time trends of water temperature at wells 29 and 14 and spring 13. Arrows indicate phases of increases (red) and decreases (blue) in temperature. The time trend of pCO_2 values, computed for the hydrothermal aquifer by Caliro et al. [2011], is plotted as a shaded area. The histogram shows the monthly number of seismic events.

Temperature variations are paralleled by changes in chemical parameters, as shown in Figures 5-7. Figure 5 shows the time trends of HCO_3^- contents, Cl^-/SO_4^{2-} ratios (for sites 13 and 29), dissolved CO_2 content (for site 29), and water temperature. The time trends of estimated pCO_2 for the hydrothermal system, computed

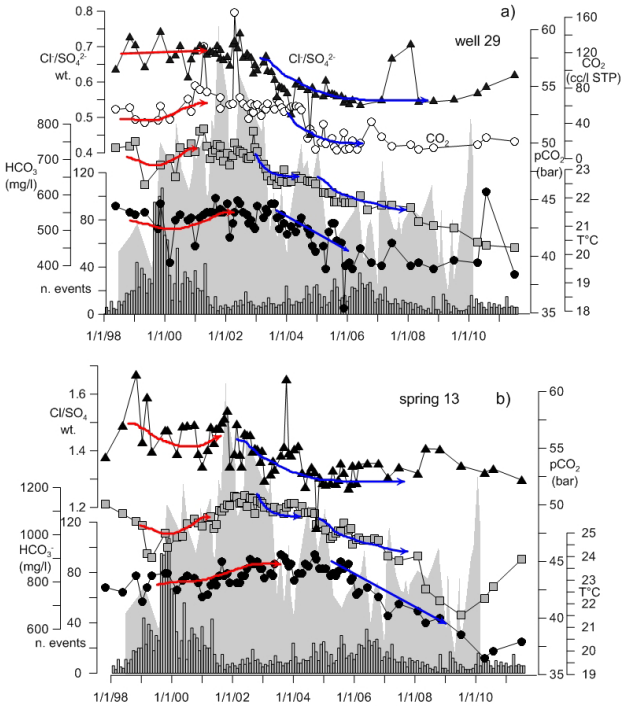

Figure 5. a) From top to bottom: time trends of the Cl^-/SO_4^{2-} ratio (triangles), dissolved CO_2 content (open circles), HCO_3^- content (squares), and water temperature (filled circles) at well 29 (Torre del Greco). b) From top to bottom: time trends of the Cl^-/SO_4^{2-} ratio (triangles), HCO_3^- content (squares), and water temperature (filled circles) at spring 13 (Torre Annunziata). Arrows indicate phases of increases (red) and decreases (blue) in the plotted parameters. The time trend of pCO_2 values, computed for the hydrothermal aquifer by Caliro et al. [2011], is plotted as a shaded area. The histogram shows the monthly number of seismic events.

from chemical data of fumarole FC2 by Caliro et al. [2011], are shown in Figure 5 as a shaded area. At well 29, the above-described time trends of temperature follow the changes in dissolved CO_2 content fairly well, with both dramatically decreasing after 2004. The HCO_3^- concentration exhibits a relative minimum coinciding with the November 1999 earthquake, and then increases along with CO_2 until 2002-2003, when a long-lasting decreasing trend begins, with an overall decrease of about 30%, which is approximately paralleled by changes in the Cl^-/SO_4^{2-} ratio. From 2006 onward, while Cl^-/SO_4^{2-} ratio remains steady, the HCO_3^- content continues decreasing. Similarly, the HCO_3^- content, temperature, and Cl^-/SO_4^{2-} ratio at site 13 follow very similar trends in the months before and after the 1999 earthquake. Thereafter, while Cl^-/SO_4^{2-} starts decreasing in 2003 before remaining steady from 2006 onward, HCO_3^- and temperature start long-lasting decreasing trends in 2004-2005 that stop in 2009-2010, with an overall decrease in the HCO_3^- content of almost 50%. The time trends of HCO_3^- contents at two other CO_2-rich sites from the Torre Annunziata area, namely wells 6 and 14 (Figure 6), confirm the above-described general pattern, characterized by relative decreases in 1999, followed by marked increases soon thereafter and new long-lasting declines from 2003 or 2004. The chemical variations observed at well 19 (Figure 7) in the Torre Annunziata area are worth noting. During 1998-2003 its HCO_3^- content shows time trends very similar to those for the other described sites. A sharp negative peak in HCO_3^- was detected in mid-2003, paralleled by comparable positive peaks in the NO_3^- content and SO_4^{2-}/HCO_3^- ratio, which last only a few months. The HCO_3^- finally declines after 2007, which is still ongoing.

Figure 8 illustrates the time trends of some geochemical parameters measured at a spring (yield <0.1 $l \cdot min^{-1}$) located on the northern flank of the volcano (Olivella spring; Figure 1). This site shows significant modifications in the water and dissolved gas chemistries and pH at the beginning of the investigated period, corresponding to the seismic sequence of October 1999, which have been attributed to the stress-induced input of acidic volcanic gases – essentially CO_2 and H_2S [Federico et al. 2004]. An overall increase in HCO_3^- is evident after the November 1999 earthquake, paralleled by a simultaneous slight decrease in pH (about 0.2 pH units

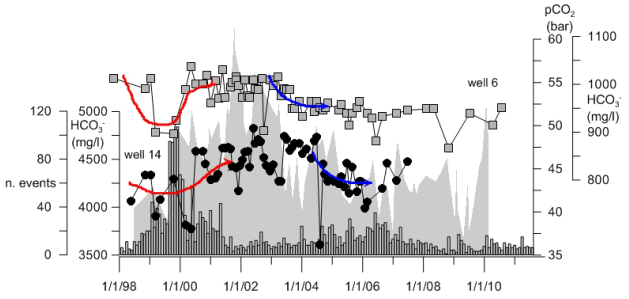

Figure 6. Time trends of HCO_3^- contents at wells 6 and 14. Arrows indicate phases of increases (red) and decreases (blue) in HCO_3^- contents. The time trend of pCO_2 values, computed for the hydrothermal aquifer by Caliro et al. [2011], is plotted as a shaded area. The histogram shows the monthly number of seismic events.

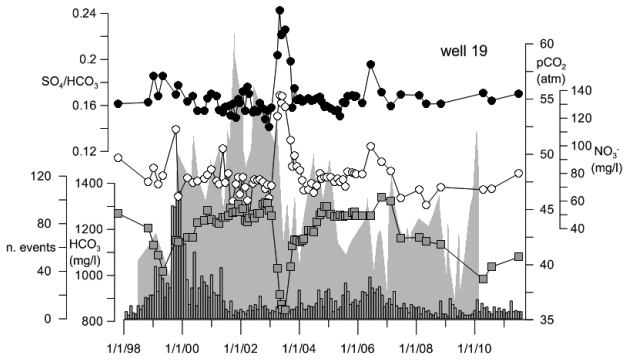

Figure 7. From top to bottom: time trends of the SO_4^{2-}/HCO_3^- ratio, NO_3^- content, and HCO_3^- content at well 19. The time trend of pCO_2 values, computed for the hydrothermal aquifer by Caliro et al. [2011], is plotted as a shaded area. The histogram shows the monthly number of seismic events.

on average) and a marked decline in the NO_3^- contents (from 60 to 20 mg·l^{-1}), which represents a marker for the shallower polluted endmember. The compositional change appears particularly evident after 2003.

Finally, time trends of dissolved CH_4/CO_2 molar ratios at selected sites (where CH_4 is detectable) – namely sites 1, 31, and 48 – are shown in Figure 9, in which the CO_2/CH_4 ratios measured at fumarole FC2 are plotted as a shaded area [Caliro et al. 2011]. We can observe relatively high CH_4/CO_2 ratios at wells 1 and 31 in 1999 (and low CO_2/CH_4 ratios at fumarole FC2), followed by very low values during 2000-2001, when CO_2 progressively increased to CH4 at the crater fumarole [Caliro et al. 2011]. Since 2002, progressively higher CH_4/CO_2 ratios have been measured in dissolved gases, remaining almost steady during the entire analyzed period. This coincides with the decrease in CO_2 concentrations at the fumaroles in the crater area.

General discussion

According to previous studies, water circulation on Mt. Vesuvius occurs in different overlapped water bodies that are characterized by different temperatures and salt contents. Higher salinity and Cl content characterize the deep-circulating and gas-charged fluids (partly contaminated by brines in the southern and western sectors), whereas the shallower endmember has a typical bicarbonate-richer composition [Federico et al. 2002, 2004]. Where the brine contribution is small (i.e., at well 6), the water salinity is almost exclusively controlled by the extent of the CO_2-driven rock-leaching and, ultimately, by the amount of interacting CO_2. Therefore, time changes in the water chemistry at the sampled sites can be reliably ascribed to changes in the mixing proportions of the deeper and shallower endmembers and to the input of CO_2.

The mixing proportions of the deeper and shallower endmembers are reliably related to the water flow rate within the aquifers, which in turn results from the variation of pressure gradients and/or permeability, according to the Darcy's law, which describes water flow in porous media. In a volcano-hydrothermal setting we can expect variations of fluid pressure to be controlled by magma degassing and/or the heat and vapor supply to hydrothermal systems [Day 1996, Reid 2004, Thomas et al. 2004]. Additionally, changes in pore pressure can be attributed to changes in the pore space volume, due to stress or self-sealing processes [Kim et al. 1997, Lazear 2009, Mortimer et al. 2011]. As suggested by Madonia et al. [2008], the crustal deformation that caused intense seismic activity in 1999 could also have changed the fluid circulation, as suggested by

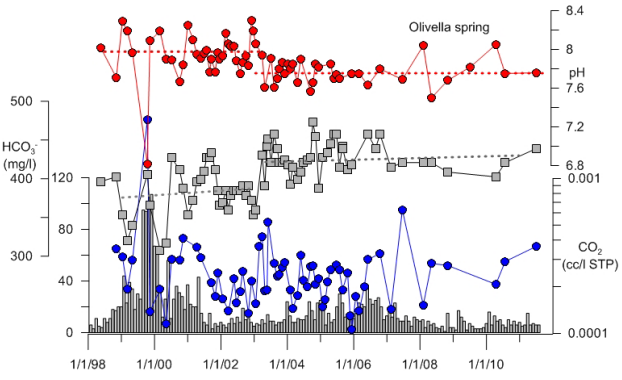

Figure 8. From top to bottom: time trends of the pH, HCO_3^- content, and dissolved CO_2 content at Olivella spring. The histogram shows the monthly number of seismic events.

water chemistry data (Figures 5-7). Analysis of the entire data record reveals a clear-cut compositional difference between the first 5 years of observations and the later period. In general, the salinity, temperature, and CO_2 and HCO_3^- contents of the wells were highest before 2003, since when (and especially after 2005) there has been a systematic decrease in these parameters characterizing the vesuvian aquifer. We suggest that the higher Cl^-/SO_4^{2-} ratios measured during 1998-2003 at wells 13 and 29, paralleled by higher temperatures and HCO_3^- and CO_2 contents, are indicative of a higher fluid pressure resulting from both the preseismic crustal deformation and the magmatic gas release corresponding to the 1999 seismic crisis. It is worth noting that the fluids emitted from fumaroles in the crater area indeed display the highest magmatic He and CO_2 contributions for typical hydrothermal gases (CH_4 and H_2O) from 2000 to 2003 [Caliro et al. 2011]. The short-lived and moderate decreases in salinity and HCO_3^- contents observed in the few months of 1999 when the largest number of seismic events occurred [Madonia et al. 2008] could be ascribed to fracture reopening and an increase in permeability caused by the intense seis-

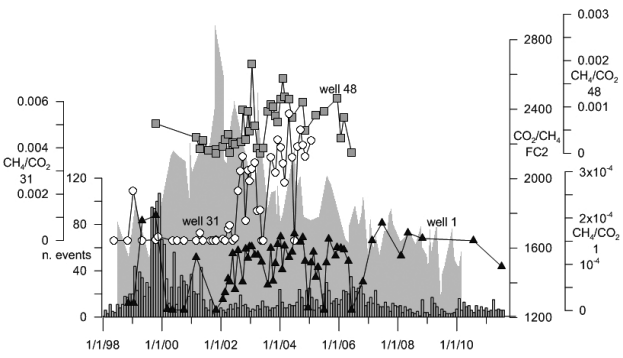

Figure 9. Time trends of CH_4/CO_2 molar ratios in the dissolved gas phase at selected sites (namely wells 1, 31, and 48). The time trend of CO_2/CH_4 molar ratios, measured at the crater fumarole by Caliro et al. [2011], is plotted as a shaded area. The histogram shows the monthly number of seismic events.

micity. As demonstrated by both field data and numerical modeling, the increase in permeability should favor the circulation of shallow fluids at greater depth [Lazear 2009], thus supporting that the shallow water endmember predominated over the deeper one.

After 2003 there was a clear-cut change in water circulation at several sites – namely 6, 13, 19, and 29, that marks an increasing contribution of the shallower Cl-poorer endmember relative to the deeper saline one. Interestingly, a dramatic change was recorded at well 19 in 2003, where a peak in the NO_3^- content (which probably reflects the contribution of shallower polluted water) is paralleled by a decrease in the HCO_3^- content.

Mid-2003 was also characterized by the occurrence of an anomalous low-frequency seismic event. Cusano et al. [2013] classified this event as a Long Period (LP) earthquake. The spectral and coda envelope analyses provided evidence of the dominance of sustained low-frequency oscillations, typical of the long-period seismicity (fluid-filled crack resonance). The presence of fluids at the depth of the vesuvian LP event (about 4 km b.s.l.) support the conceptual geochemical model of the volcanic system of Mt. Vesuvius depicted by Caliro et al. [2011], in which the brine sources were positioned just shallower than the LP hypocenter.

On these grounds and taking into account the variations in the groundwater chemistry described in the present work, we suggest that the LP seismic event that occurred in summer 2003 could have caused a pressure decrease that was sustained until that moment by the degassing of magmatic volatiles (mostly CO_2), as observed by Caliro et al. [2011]. The pressure drop could have increased the circulation of shallower fluids into a deeper aquifer, thus explaining the change in chemical composition and the decrease in the saline contents of fluids at the monitored sites.

While the water composition indicates the dominant contribution of shallow water since 2003, the temperature and/or CO_2 and HCO_3^- concentrations at some wells (namely wells 26, 13, 14, and 29) remained high until 2005-2006. This would support inputs of water vapor and CO_2 into the shallow aquifer, and we cannot exclude that this is also an effect of a reduced confining pressure in the hydrothermal aquifer caused by the 2003 event. Otherwise, as observed in Figure 8, an increase in HCO_3^- content from 2003 at Olivella spring is paralleled by a slight reduction in pH (of about 0.2 units), which supports a subsequent higher input of CO_2.

The time trends of CH_4/CO_2 ratios measured at selected wells (where dissolved CH_4 is detectable, at $>10^{-5}$ cc·l^{-1} STP) are compatible with the CO_2/CH_4 ratios measured at the crater fumarole [Caliro et al. 2011], and support that the contribution from the hydrothermal vapor has been greater than that from the magmatic CO_2-richer gases since 2003. Additionally, the CH_4/CO_2 ratios in groundwater can vary due to a reduced flux of deep gases, since these gas species have different solubilities in water. Indeed, partial dissolution of gases in water can modify the original gas composition as an effect of the specific solubility coefficients and the relative amount of residual gas, according to a Rayleigh-type fractionation [Federico et al. 2002, Caracausi et al. 2003, Capasso et al. 2005]:

$$\left(\frac{[CH_4]}{[CO_2]}\right)_{liq} = \left(\frac{K_{H,CO_2}}{K_{H,CH_4}}\right)\cdot\left(\frac{[CH_4]}{[CO_2]}\right)_{gas,in}\cdot\left(\frac{m_{CO_2}}{m_{CO_2,in}}\right)^{\left(\frac{K_{H,CO_2}}{K_{H,CH_4}}-1\right)} \quad (1)$$

where subscripts liq, gas, and in indicate the liquid phase, gas phase, and initial condition, respectively, K_{H,CH_4} and K_{H,CO_2} are Henry's constants for the gas species CH_4 and CO_2, and m_{CO_2} is the number of moles of CO_2. Given the large difference in Henry's constant between CH_4 and CO_2 (39,900 and 1667 atm·mol·mol^{-1}, respectively, at 25°C [Wilhelm et al. 1977]), the exponent in Equation (1) is <0. Therefore, a dramatic reduction in the fraction of the residual gas (i.e., $\frac{m_{CO_2}}{m_{CO_2,in}} \ll 1$) due to the progressive dissolution in water can be expected to increase the CH_4/CO_2 ratios.

The lower salinities, temperatures, and CO_2 contents from 2006 onward clearly indicate a reduced input of volcanic volatiles and lower fluid pressure in the volcanic aquifer.

Conclusions

The chemical analyses of water and dissolved gas samples obtained during 1998-2011 indicate that the geochemical behavior of the vesuvian aquifer is strictly controlled by variations in the input of deep-seated volcanic gases and in the stress field. The changes in the stress field, which were responsible for the seismic crisis of 1999, and the almost simultaneous increased input of CO_2-rich vapor, significantly affected the recorded composition and temperature of the groundwater. Indeed, an increase in fluid pressure characterized the period from 1998 to 2003, inducing a change in water circulation and the predominance of a deeper water endmember over the shallower one in the vesuvian aquifer. Moreover, the groundwater temperature and dissolved carbon contents (in terms of both HCO_3^- and CO_2) are clearly indicative of inputs of CO_2 and steam until 2005-2006. The termination of the phase of intense deep degassing, as observed in the crater area and in groundwater, is associated with a pressure decrease evident in the water chemistry and paralleled by a peculiar seismic event that was recorded in July 2003. The recent observations of low salinity, temperature,

and dissolved carbon contents in groundwater provide strong evidence for reduced pressure in the volcano-hydrothermal system at Mt. Vesuvius. The variations of specific geochemical parameters can therefore be ascribed to either stress-induced changes in water circulation or changes in the inputs of deep gases. The multidisciplinary approach and the comparison with geophysical signals applied in this study have made it possible to ascertain the roles of the stress field and the degassing of hydrothermal/magmatic systems in producing the observed changes. This has implications when evaluating the reciprocal effects of tectonics and volcanic/hydrothermal activity, which is an open field of investigation.

References

Aiuppa, A., A. Caleca, C. Federico, S. Gurrieri and M. Valenza (2004). Diffuse degassing of carbon dioxide at Somma-Vesuvius volcanic complex (Southern Italy) and its relation with regional tectonics, J. Volcanol. Geoth. Res., 133, 55-79.

Aiuppa, A., C. Federico, P. Allard, S. Gurrieri and M. Valenza (2005). Trace metal modelling of groundwater-gas-rock interactions in a volcanic aquifer: Mount Vesuvius (Southern Italy), Chem. Geol., 216, 289-311.

Andronico, D., G. Calderoni, R. Cioni, A. Sbrana, R. Sulpizio and R. Santacroce (1995). Geological map of Somma-Vesuvius volcano, Periodico di Mineralogia, 64 (1-2), 77-78.

Ayuso, R.A., B. De Vivo, G. Rolandi, R.R. Seal II and A. Paone (1998). Geochemical and isotopic (Nd-Pb-Sr-O) variations bearing on the genesis of volcanic rocks from Vesuvius, Italy, J. Volcanol. Geoth. Res., 82, 53-78.

Belkin, H.E., C.R.J. Kilburn and B. De Vivo (1993). Sampling and major element chemistry of the recent (A.D. 1631-1944) Vesuvius activity, J. Volcanol. Geoth. Res., 58, 273-290.

Bertagnini, A., R. Cioni, E. Guidoboni, M. Rosi, A. Neri and E. Boschi (2006). Eruption early warning at Vesuvius: The A.D. 1631 lesson, Geophys. Res. Lett., 33, L18317; doi:10.1029/2006GL027297.

Biagi, P.F., L. Castellana, R. Piccolo, A. Minafra, G. Maggipinto, A. Ermini, V. Capozzi, G. Perna, Y.M. Khatkevich and E.I. Gordeev (2004). Disturbances in groundwater chemical parameters related to seismic and volcanic activity in Kamchatka (Russia), Nat. Hazards Earth Syst. Sci., 4, 535-539.

Bianco, F., M. Castellano, G. Milano, G. Ventura, G. and Vilardo (1998). The Somma-Vesuvius stress field induced by regional tectonics: Evidences from seismological and mesostructural data, J. Volcanol. Geoth. Res., 82, 199-218; doi:10.1016/S0377-0273(97)00065-6.

Bianco, F., P. Cusano, S. Petrosino, M. Castellano, C. Buonocunto, M. Capello and E. Del Pezzo (2005). Small-aperture Array for Seismic Monitoring of Mt. Vesuvius, Seismol. Res. Lett., 76, 344-355; doi: 10.1785/gssrl.76.3.344.

Caliro, S., C. Panichi and D. Stanzione (1998). Baseline study of the isotopic and chemical composition of waters associated with the Somma-Vesuvius volcanic system, Acta Vulcanol., 10, 19-25.

Caliro, S., G. Chiodini, R. Avino, C. Cardellini and F. Frondini (2005). Volcanic degassing at Somma-Vesuvio (Italy) inferred by chemical and isotopic signatures of groundwater, Appl. Geochem., 20, 1060-1076.

Caliro, S., G. Chiodini, R. Avino, C. Minopoli and B. Bocchino (2011). Long time-series of chemical and isotopic compositions of Vesuvius fumaroles: evidence for deep and shallow processes, Annals of Geophysics, 54 (2), 137-149; doi:10.4401/ag-5034.

Capasso, G., and S. Inguaggiato (1998). A simple method for the determination of dissolved gases in natural waters. An application to thermal waters from Vulcano Island, Appl. Geochem., 13, 631-642.

Capasso, G., M.L. Carapezza, C. Federico, S. Inguaggiato and A. Rizzo (2005). Geochemical monitoring of the 2002-2003 eruption at Stromboli volcano (Italy): precursory changes in the carbon and helium isotopic composition of fumarole gases and thermal waters, Bull. Volcanol., 68, 118-134; doi: 10.1007/s00445-005-0427-5.

Caracausi, A., F. Italiano, A. Paonita and A. Rizzo (2003). Evidence of deep magma degassing and ascent by geochemistry of peripheral gas emissions at Mount Etna (Italy): Assessment of the magmatic reservoir pressure, J. Geophys. Res., 108 (B10), 2463; doi:10.1029/2002JB002095.

Castellano, M., D. Galluzzo, M. La Rocca and M. Capello (2012). Lo studio dei vulcani attivi e delle strutture crostali con reti sismiche temporanee: storia, evoluzione e prospettive della Rete Sismica Mobile dell'Osservatorio Vesuviano (INGV), Quaderni di Geofisica, INGV, no. 97, 51 pp. ISSN:1590-2595.

Celico, P., D. Stanzione, L. Esposito, M.R. Ghiara, V. Piscopo, S. Caliro and P. La Gioia (1998). Caratterizzazione idrogeologica e idrogeochimica dell'area Vesuviana, Boll. Soc. Geol. It., 117, 3-20.

Chouet, B.A. (1996). Long-period volcano seismicity: its sources and use in eruption forecasting, Nature, 380 (6572), 309-316; doi:10.1038/380309a0.

Cioni, R., P. Marianelli and R. Santacroce (1998). Thermal and compositional evolution of the shallow

magma chambers of Vesuvius: Evidence from pyroxene phenocrysts and melt inclusions, J. Geophys. Res., 103, 18277-18294; doi:10.1029/98JB01124.

Corniello, A., R. De Riso and D. Ducci (1990). Idrogeologia e idrogeochimica della Piana Campana, Mem. Soc. Geol. It., 45, 351-360.

Cusano P., S. Petrosino, F. Bianco and E. Del Pezzo (2013). The first Long Period earthquake detected in the background seismicity at Mt. Vesuvius, Annals of Geophysics, 56 (4), S0440; doi:10.4401/ag-6447.

Day, S.J. (1996). Hydrothermal pore fluid pressure and the stability of porous, permeable volcanoes, In: W.C. McGuire, A.P. Jones and J. Neuberg (eds.), Volcano Instability on the Earth and Other Planets, Geol. Soc. London, Spec. Publ. no. 110, 77-93.

Del Pezzo, E., G. Iannaccone, M. Martini, and R. Scarpa (1983). The 23 November, 1980 Southern Italy Earthquake, Bull. Seismol. Am., 73 (1), 187-200.

Del Pezzo, E., F. Bianco and G. Saccorotti (2004). Seismic source dynamics at Vesuvius volcano, Italy, J. Volcanol. Geoth. Res., 133, 23-39; doi:10.1016/S0377-0273(03)00389-5.

De Vivo, B., and G. Rolandi, eds. (2001). Mt. Somma-Vesuvius and volcanism of the Campanian Plain, Mineral. Petrol., 73, 233 pp.

Federico, C., A. Aiuppa, P. Allard, S. Bellomo, P. Jean-Baptiste, F. Parello and M. Valenza (2002). Magma-derived gas influx and water-rock interactions in the volcanic aquifer of Mt. Vesuvius, Italy, Geochim. Cosmochim. Acta, 66, 963-981.

Federico, C., A. Aiuppa, R. Favara, S. Gurrieri and M. Valenza (2004). Geochemical monitoring of groundwaters (1998-2001) at Vesuvius volcano (Italy), J. Volcanol. Geoth. Res., 133, 81-104, doi: 10.1016/S0377-0273(03)00392-5.

Frondini, F., G. Chiodini, S. Caliro, C. Cardellini, D. Granieri and G. Ventura (2004). Diffuse CO_2 degassing at Vesuvio, Italy, Bull. Volcanol., 66, 642-651; doi:10.1007/s00445-004-0346-x.

Giudicepietro, F., M. Orazi, G. Scarpato, R. Peluso, L. D'Auria, P. Ricciolino, D. Lo Bascio, A. M. Esposito, G. Borriello, M. Capello, A. Caputo, C. Buonocunto, W. De Cesare, G. Vilardo and M. Martini (2010). Seismological Monitoring of Mount Vesuvius (Italy): More than a Century of Observations, Seismol. Res. Lett., 81 (4), 625-634; doi: 10.1785/gssrl.81.4.625.

Gottsmann, J., R. Carniel, N. Coppo, L. Wooller, S. Hautmann and H. Rymer (2007). Oscillations in hydrothermal systems as a source of periodic unrest at caldera volcanoes: Multiparameter insights from Nisyros, Greece, Geophys. Res. Lett., 34, L07307; doi:10.1029/2007GL029594.

Hill, D.P., F. Pollitz and C. Newhall (2002). Earthquake-volcano interactions, Physics Today, 55 (11), 41-47.

Hurwitz, S., and M.J.S. Johnston (2003). Groundwater level changes in a deep well in response to a magma intrusion event on Kilauea Volcano, Hawai'i, Geophys. Res. Lett., 30 (22), 2173; doi:10.1029/2003GL018676.

Kim, J.M., R.R. Parizek and D. Elsworth (1997). Evaluation of fully coupled strata deformation and groundwater flow in response to longwall mining, International Journal of Rock Mechanics and Mining Sciences, 34, 1187-1199.

Koizumi, N., Y. Kitagawa, N. Matsumoto, M. Takahashi, T. Sato, O. Kamigaichi and K. Nakamura (2004). Preseismic groundwater level changes induced by crustal deformations related to earthquake swarms off the east coast of Izu Peninsula, Japan, Geophys. Res. Lett., 31, L10606; doi:10.1029/2004GL019557.

Lazear, G.D. (2009). Fractures, convection and underpressure: hydrogeology on the southern margin of the Piceance basin, west-central Colorado, USA, Hydrogeol. J., 17, 641-664.

Lomax, A., J. Virieux, P. Volant and C. Berge (2000). Probabilistic earthquake location in 3D and layered models: Introduction of a Metropolis-Gibbs method and comparison with linear locations, In: C.H. Rabinowitz and N. Rabinowitz (eds.), Advances in Seismic Event Location Thurber, Springer, Amsterdam, 101-134.

Madonia, P., C. Federico, P. Cusano, S. Petrosino, A. Aiuppa and S. Gurrieri (2008). Crustal dynamics of Mount Vesuvius from 1998 to 2005: Effects on seismicity and fluid circulation, J. Geophys. Res., 113, B05206; doi:10.1029/2007JB005210.

Marzocchi, W., R. Scandone and F. Mulargia (1993). The tectonic setting of Mount Vesuvius and the correlation between its eruptions and the earthquakes of the southern Apennines, J. Volcanol. Geoth. Res., 58, 27-41, doi:10.1016/0377-0273(93)90100-6.

Mortimer, L., A. Aydin, C.T. Simmons and A.J. Love (2011). Is in situ stress important to groundwater flow in shallow fractured rock aquifers?, J. Hydrol., 399, 185-200.

Newhall, C.G., S.E. Albano, N. Matsumoto and T. Sandoval (2001). Roles of groundwater in volcanic unrest, J. Geol. Soc. Philipp., 56, 69-84.

Principe, C., D. Brocchini and M. Perillo (1999). The 'Cognoli di Trocchia' volcano and Monte Somma growth, Plinius, 22, 316-317.

Reid, M.E. (2004). Massive collapse of volcano edifices triggered by hydrothermal pressurization, Geology, 32, 373-376.

Roeloffs, E., M. Sneed, D.L. Galloway, M.L. Sorey, C.D.

Farrar, J.F. Howle and J. Hughes (2003). Water-level changes induced by local and distant earthquakes at Long Valley caldera, California, J. Volcanol. Geoth. Res., 127, 269-303; doi:10.1016/S0377-0273(03)00173-2.

Santacroce, R., ed. (1987). Somma-Vesuvius, Quaderni de "La Ricerca Scientifica", CNR, 114 (Progetto finalizzato Geodinamica, Monografie finali, 8), 251 pp.

Santacroce, R., R. Cioni, L. Civetta, P. Marianelli and N. Métrich (1994). How Vesuvius works, Atti dei Convegni Lincei, 112, 185-196.

Saccorotti, G., G. Ventura and G. Vilardo (2002). Seismic swarms related to diffusive processes: The case of Somma-Vesuvius volcano, Italy, Geophysics, 67 (1), 199-203; doi:10.1190/1.1451551.

Scandone, R., F. Bellucci, L. Lirer and G. Rolandi (1991). The structure of the Campanian Plain and the activity of the Neapolitan volcanoes (Italy), J. Volcanol. Geoth. Res., 48 (1-2), 1-31; doi:10.1016/0377-0273(91)90030-4.

Scarpa, R., F. Tronca, F. Bianco and E. Del Pezzo (2002). High resolution velocity structure beneath Mount Vesuvius from seismic array data, Geophys. Res. Lett., 29 (21), 2040; doi:10.1029/2002GL015576.

Shibata, T., and F. Akita (2001). Precursory changes in well water level prior to the March, 2000 eruption of Usu volcano, Japan, Geophys. Res. Lett., 28, 1799-1802.

Thomas, M.E., N. Petford and E.N. Bromhead (2004). The effect of internal gas pressurization on volcanic edifice stability: evolution towards a critical state, Terra Nova, 16, 312-317.

Ventura, G., and G. Vilardo (1999). Slip tendency analysis of the Vesuvius faults: Implications for the seismotectonic and volcanic hazard assessment, Geophys. Res. Lett., 26 (21), 3229-3232; doi:10.1029/1999GL005393.

Wilhelm, E., R. Battino and R.J. Wilckock (1977). Low pressure solubility of gases in liquid water, Chem. Rev., 77, 219-262.

Zollo, A., W. Marzocchi, P. Capuano, A. Lomax and G. Iannaccone (2002). Space and time behavior of seismic activity at Mt. Vesuvius volcano, southern Italy, Bull. Seismol. Soc. Am., 92 (2), 625-640; doi:10.1785/0120000287.

*Corresponding author: Cinzia Federico,
Istituto Nazionale di Geofisica e Vulcanologia, Sezione di Palermo, Palermo, Italy; email: c.federico@pa.ingv.it.

Site 6														
Date (mo/yr)	T (°C)	pH	Eh (mV)	Na^+ (mg/l)	K^+ (mg/l)	Mg^{2+} (mg/l)	Ca^{2+} (mg/l)	Cl^- (mg/l)	NO_3^- (mg/l)	SO_4^{2-} (mg/l)	HCO_3^- (mg/l)	TDS (mg/l)	CH_4 cc/l STP	CO_2 cc/l STP
11/98	16.9	5.9	-270	142	252	83	58	209	<0.1	36	990	1770	5.E-01	1060
1/99	16.8	5.9	-130	136	242	83	57	202	<0.1	39	1010	1770	1.E+00	1090
3/99	16.4	6.1	-90	141	258	81	57	210	0.5	39	850	1710	<0.0001	520
10/99	16.7	5.8	-120	144	252	90	59	168	0.5	41	990	1660	5.E-01	1200
11/99	16.9	5.9	-280	149	243	89	64	170	0.3	34	990	1710	7.E-01	943
3/00	16.8	6.1	-275	146	250	84	59	168	4.3	36	990	1730	n.m.	n.m.
5/00	16.8	5.9	-200	151	259	89	56	165	1.9	31	1040	1790	2.E-01	990
7/00	17.1	5.8	-180	139	240	92	67	181	1.5	44	1030	1770	2.E-01	1230
10/00	16.7	5.7	-210	136	241	92	52	149	<0.1	34	1000	1680	n.d.	1520
11/00	16.6	5.8	-160	134	235	85	54	171	<0.1	38	1020	1740	4.E-01	1240
1/01	16.5	6.0	n.m.	137	251	75	57	168	0.2	36	960	1690	5.E-02	740
3/01	16.6	5.9	n.m.	144	242	78	71	170	<0.1	35	1010	1740	6.E-04	970
4/01	16.7	5.9	-50	137	237	84	55	155	3.0	40	970	1700	5.E-01	950
5/01	17.1	5.7	24	134	230	88	59	148	0.2	34	1030	1770	7.E-02	1190
6/01	17.1	5.9	57	135	234	88	57	174	0.2	45	970	1700	<0.0001	830
8/01	16.7	5.9	-85	138	241	89	62	179	5	45	990	1750	n.m.	n.m.
9/01	16.6	5.9	60	144	243	89	66	171	4.3	46	1000	1760	n.m.	n.m.
10/01	16.7	5.9	-34	144	239	93	66	165	3.7	47	1020	1770	4.E-02	850
11/01	16.6	5.8	25	143	237	90	64	169	<0.1	35	1010	1750	<0.0001	450
12/01	16.7	6.0	15	134	241	84	64	160	<0.1	33	1000	1710	n.m.	n.m.
1/02	16.7	5.9	-130	136	234	81	60	177	<0.1	59	970	1720	1.E-01	1030
2/02	16.7	6.1	30	141	236	81	58	144	<0.1	39	1010	1710	6.E-02	1030
3/02	16.4	5.9	-200	142	248	83	61	173	<0.1	43	980	1730	2.E-01	680
4/02	16.8	5.8	-36	144	238	89	59	187	<0.1	35	970	1720	3.E-01	830
5/02	16.9	5.9	-38	143	236	86	58	168	<0.1	59	1010	1760	5.E-01	870
6/02	16.9	6.0	-20	149	249	87	62	174	<0.1	47	990	1760	1.E-01	820
7/02	17.5	5.9	-200	149	248	87	62	171	<0.1	48	990	1750	5.E-01	850
9/02	17.4	5.9	-180	139	236	80	56	168	<0.1	36	1010	1730	6.E-01	820
9/02	16.7	5.9	-180	138	235	78	55	168	<0.1	37	900	1610	8.E-01	850
12/02	16.3	5.8	-90	138	239	79	55	146	<0.1	39	1010	1710	4.E-04	710
1/03	16.50	5.6	-110	141	236	81	52	163	3	33	1000	1700	1.E-01	770
3/03	16.9	5.8	-120	158	248	86	57	170	<0.1	44	1020	1780	2.E-04	760
4/03	16.9	5.9	-150	153	243	85	55	210	<0.1	37	980	1760	1.E-04	830
5/03	17.3	5.9	-210	139	248	84	53	172	<0.1	36	990	1720	1.E-04	710

Table A1 (continues on next page).

Site 6														
Date (mo/yr)	T (°C)	pH	Eh (mV)	Na^+ (mg/l)	K^+ (mg/l)	Mg^{2+} (mg/l)	Ca^{2+} (mg/l)	Cl^- (mg/l)	NO_3^- (mg/l)	SO_4^{2-} (mg/l)	HCO_3^- (mg/l)	TDS (mg/l)	CH_4 cc/l STP	CO_2 cc/l STP
6/03	17.6	n.m.	-180	144	252	87	55	174	<0.1	38	990	1740	2.E-03	670
7/03	17.5	6.0	-190	140	248	85	56	182	<0.1	47	990	1750	n.m.	n.m.
8/03	17.3	6.0	-170	136	241	89	54	190	<0.1	58	990	1760	3.E-02	820
9/03	17	5.9	-110	135	243	91	60	172	0.19	60	950	1710	3.E-01	860
10/03	16.9	5.8	-250	138	247	87	54	163	<0.1	57	950	1700	3.E-01	1000
12/03	16.6	5.9	-120	135	239	83	60	174	<0.1	37	960	1690	3.E-01	900
01/04	16.5	5.5	-210	132	234	82	58	165	<0.1	49	930	1650	6.E-01	800
4/04	16.7	5.7	-290	138	244	82	58	176	4.34	38	960	1700	3.E-01	800
5/04	17	5.9	-140	134	241	84	58	176	<0.1	47	940	1680	6.E-02	780
6/04	16.9	n.m.	-110	135	245	87	60	181	<0.1	44	960	1720	5.E-01	860
8/04	n.m.	n.m.	n.m.	137	243	89	59	192	<0.1	56	950	1730	5.E-01	790
9/04	16.9	5.8	140	142	254	90	61	201	<0.1	72	950	1770	4.E-01	770
10/04	16.8	5.9	-85	127	246	79	63	178	<0.1	61	950	1710	5.E-01	840
11/04	16.7	5.9	-85	138	243	83	59	172	<0.1	42	960	1700	8.E-01	840
3/05	16.8	5.8	-100	138	254	86	50	176	<0.1	46	950	1700	3.E-01	850
4/05	16.7	5.9	43	127	227	81	58	165	<0.1	38	960	1650	2.E-01	760
6/05	16.9	5.8	-180	137	244	91	64	195	<0.1	54	940	1730	4.E-01	730
7/05	16.9	5.9	-160	136	241	91	63	202	<0.1	67	920	1720	4.E-04	650
8/05	16.9	n.m.	n.m.	137	245	89	62	189	<0.1	67	940	1730	4.E-01	760
10/05	16.8	n.m.	n.m.	135	243	88	63	189	<0.1	44	950	1710	5.E-01	770
11/05	16.4	5.7	n.m.	134	241	86	63	172	<0.1	41	960	1700	5.E-01	790
3/06	16.7	n.m.	n.m.	141	242	88	62	207	<0.1	50	940	1730	7.E-01	820
6/06	17	5.7	n.m.	139	247	90	65	217	<0.1	101	880	1740	4.E-01	710
2/07	16.7	n.m.	n.m.	141	244	93	66	225	<0.1	38	940	1750	n.m.	n.m.
6/07	n.m.	n.m.	n.m.	138	239	95	70	218	<0.1	41	950	1750	5.E-01	820
2/08	16.8	5.9	-200	140	245	92	63	214	<0.1	40	950	1740	3.E-01	840
5/08	16.9	n.m.	-50	142	248	99	71	235	<0.1	35	950	1780	n.m.	n.m.
10/08	17.0	5.9	-240	127	218	86	63	226	<0.1	56	870	1640	n.m.	n.m.
7/09	17.0	6.0	-220	135	245	94	63	232	<0.1	48	940	1760	n.m.	n.m.
4/10	17.1	n.m.	-170	127	218	92	67	191	<0.1	47	920	1660	n.m.	n.m.
7/10	17.5	5.9	n.m.	130	237	92	63	221	<0.1	37	950	1730	3.E-01	760

Table A1 (continued from previous page).

Site 13												
Date (mo/yr)	T (°C)	pH	Eh (mV)	Na^+ (mg/l)	K^+ (mg/l)	Mg^{2+} (mg/l)	Ca^{2+} (mg/l)	Cl^- (mg/l)	NO_3^- (mg/l)	SO_4^{2-} (mg/l)	HCO_3^- (mg/l)	TDS (mg/l)
5/98	22.5	6.0	-90	179	328	105	188	360	20.6	242	1090	2490
11/98	23.2	6.0	-100	185	350	101	167	460	<0.1	275	1060	2590
1/99	22.1	6.2	-70	175	327	101	180	390	3.2	273	1040	2490
3/99	22.7	5.9	-110	180	330	101	174	420	0.4	262	920	2390
5/99	23.2	5.9	-260	170	333	95	166	360	0.2	256	900	2290
10/99	23.3	6.7	-110	173	342	88	164	340	3.5	231	1010	2320
11/99	23.3	6.0	-250	159	321	91	149	320	6.8	219	950	2240
3/00	22.6	6.0	-270	171	307	92	169	340	5.0	247	990	2320
5/00	23.0	6.0	-160	179	326	96	157	380	3.1	255	990	2360
7/00	23.2	6.0	-60	178	324	104	186	400	3.1	268	1050	2500
10/00	23.1	6.0	-200	200	360	112	179	420	<0.1	281	1070	2620
11/00	22.9	5.9	-180	171	306	96	180	380	1.8	274	1050	2450
1/01	22.3	6.0	n.m.	167	340	95	223	390	<0.1	265	1040	2480
3/01	22.4	6.0	n.m.	185	325	105	191	390	<0.1	280	1070	2560
4/01	22.8	6.0	-35	177	325	107	192	390	<0.1	263	1080	2530
5/01	23.0	6.0	34	181	326	109	191	400	<0.1	282	1030	2520
6/01	22.8	5.93	44	184	335	108	186	430	5.2	293	1040	2580
7/01	23.2	5.99	-220	206	362	111	192	460	6.7	310	1100	2740
8/01	23.8	5.74	-100	216	365	116	184	470	5.0	312	1100	2760
9/01	23.2	5.93	-100	215	372	117	194	490	4.3	324	1110	2830
10/01	23.3	5.93	-100	227	386	123	198	480	1.2	313	1130	2860
11/01	22.9	5.95	55	205	353	120	200	440	<0.1	329	1120	2770
01/02	n.m.	5.8	-90	217	390	119	233	470	<0.1	341	1160	2940
02/02	22.9	5.8	-70	220	376	112	206	480	30.4	323	1160	2880
03/02	22.9	5.9	-200	227	400	119	224	500	<0.1	360	1130	2960
04/02	23.2	5.9	-150	214	386	116	230	450	<0.1	335	1140	2870
05/02	23.2	6.0	-20	224	384	119	207	460	<0.1	314	1170	2870
06/02	23.5	6.1	-6	223	382	112	216	460	<0.1	317	1120	2830
07/02	23.9	6.1	-190	231	390	114	210	470	<0.1	325	1160	2900
08/02	23.7	6.0	-350	231	393	112	194	470	<0.1	334	1150	2880
09/02	23.7	6.0	-144	228	389	110	198	470	<0.1	332	1090	2820
10/02	23.8	5.9	-140	233	398	112	201	470	<0.1	332	1140	2890
12/02	23.5	6.1	-59	227	381	111	198	450	<0.1	331	1140	2840
12/02	23.5	5.9	12	214	378	107	195	410	<0.1	295	1130	2730
01/03	23.1	5.9	-43	202	343	100	208	410	<0.1	318	1120	2700
03/03	23.3	6.0	-83	225	356	104	203	410	<0.1	312	1110	2730
04/03	23.2	6.0	-190	217	351	102	207	430	7	318	1100	2730
05/03	23.7	n.m.	-140	196	360	98	212	410	4	306	1120	2700

Table A2 (continues on next page).

Site 13												
Date (mo/yr)	T (°C)	pH	Eh (mV)	Na^+ (mg/l)	K^+ (mg/l)	Mg^{2+} (mg/l)	Ca^{2+} (mg/l)	Cl^- (mg/l)	NO_3^- (mg/l)	SO_4^{2-} (mg/l)	HCO_3^- (mg/l)	TDS (mg/l)
08/03	24.1	6.1	-110	205	380	104	197	430	3	314	1110	2740
09/03	24	6.1	-200	199	367	115	202	440	6	310	1090	2720
10/03	23.8	6.1	-93	203	369	108	220	480	7	292	1120	2790
11/03	23.6	6.0	-90	214	387	105	198	450	6	320	1130	2800
12/03	23.7	6.0	-62	208	385	100	205	420	5	304	1140	2760
01/04	23.0	5.9	-200	205	373	104	205	420	5	299	1140	2740
03/04	23.3	5.8	-30	184	335	95	214	390	0	272	1090	2570
04/04	23.3	5.8	-30	185	330	93	212	370	6	276	1120	2580
05/04	23.7	6.0	-27	180	324	89	210	340	2	268	1090	2500
06/04	23.6	n.m.	-82	184	337	94	204	370	19	281	1090	2560
08/04	n.m.	n.m.	n.m.	203	360	97	200	400	2	297	1100	2650
09/04	24.1	6.1	-90	203	368	96	191	400	2	300	1090	2640
10/04	23.9	6.0	-70	171	330	75	179	290	16	253	1040	2340
11/04	23.5	5.9	-38	169	310	79	180	300	12	232	1050	2320
12/04	23.5	5.9	-18	177	322	86	193	340	4	261	1050	2420
01/05	23.5	n.m.	-37	181	322	86	186	340	4	265	1020	2400
03/05	23.2	6.0	-60	162	316	78	179	300	7	234	980	2250
04/05	23.3	5.8	70	157	288	74	169	290	9	214	990	2180
05/05	23.2	5.9	-3.5	172	314	80	181	310	<0.1	238	1010	2300
06/05	23.4	5.9	-92	183	330	85	186	340	<0.1	263	1020	2400
07/05	23.8	5.9	-36	179	326	84	179	340	<0.1	248	1010	2360
08/05	23.5	n.m.	n.m.	193	346	91	189	360	<0.1	271	1050	2500
10/05	23.7	n.m.	n.m.	177	320	81	177	320	<0.1	252	1020	2340
11/05	23	n.m.	n.m.	182	330	86	182	330	<0.1	254	1030	2390
12/05	23.1	n.m.	n.m.	167	293	79	177	310	<0.1	228	960	2210
01/06	22.4	n.m.	n.m.	175	305	83	183	320	<0.1	251	980	2300
03/06	22.5	n.m.	n.m.	183	319	86	184	350	<0.1	262	980	2370
06/06	22.7	5.9	n.m.	161	294	80	186	310	<0.1	228	980	2230
10/06	22.3	5.8	-40	161	294	80	186	310	<0.1	228	980	2230
02/07	21.5	n.m.	n.m.	145	259	68	166	250	<0.1	192	910	1990
06/07	22.0	5.9	-20	136	242	63	154	220	<0.1	165	890	1870
02/08	21.7	5.8	-35	128	230	60	138	200	<0.1	155	910	1824
05/08	21.2	6.8	-150	116	213	52	130	190	<0.1	137	770	1610
10/08	21.4	5.8	-230	107	190	47	118	170	<0.1	119	720	1470
07/09	20.7	5.9	-200	88	167	41	108	130	<0.1	97	660	1290
04/10	19.7	5.8	n.m.	88	163	55	154	180	<0.1	132	730	1500
07/10	20.0	5.6	n.m.	103	196	59	165	220	<0.1	164	780	1690
07/11	20.4	5.9	40	142	247	68	181	280	<0.1	212	900	2020

Table A2 (continued from previous page).

Site 14														
Date (mo/yr)	T (°C)	pH	Eh (mV)	Na^+ (mg/l)	K^+ (mg/l)	Mg^{2+} (mg/l)	Ca^{2+} (mg/l)	Cl^- (mg/l)	NO_3^- (mg/l)	SO_4^{2-} (mg/l)	HCO_3^- (mg/l)	TDS (mg/l)	CH_4 cc/l STP	CO_2 cc/l STP
5/98	23.3	6.3	-170	530	410	760	620	2000	<0.1	88	4060	8470	0.010	500
11/98	23.3	6.4	-260	540	415	770	620	2200	2.4	86	4340	8980	0.500	890
1/99	23.2	6.4	-70	560	413	810	590	2020	7.1	88	4340	8810	0.180	740
3/99	23.1	6.4	-90	530	433	760	610	1970	0.7	82	3910	8300	0.190	1010
5/99	23.5	6.4	-260	530	413	720	590	1830	5.9	87	4080	8470	0.080	680
10/99	23.2	6.4	-150	510	429	830	550	1880	1.7	82	4290	8550	0.130	730
3/00	22.6	6.5	-200	520	420	790	410	2100	21.0	114	3820	8180	0.070	900
5/00	22.9	6.9	-250	540	414	830	400	2080	6.8	113	3770	7990	0.190	1180
7/00	23.4	6.4	-200	530	401	770	670	1980	17.0	105	4590	9120	0.001	660
10/00	23.0	6.3	-130	560	422	790	510	1880	<0.1	77	4590	8970	0.230	1030
11/00	22.3	6.3	-80	510	387	790	550	1980	<0.1	77	4450	8860	0.450	1090
1/01	21.8	6.6	n.m.	560	352	800	730	2110	1.2	71	4290	8660	0.350	860
3/01	22.1	6.5	n.m.	530	406	780	570	1810	1.2	80	4300	8420	0.430	820
4/01	22.1	6.4	-90	510	392	840	610	1860	7.3	95	4340	8640	0.340	800
5/01	22.4	6.2	-80	500	392	790	570	1910	0.8	71	4620	8890	0.330	960
6/01	23.1	6.4	-58	510	381	810	680	2040	5.0	84	4620	9120	0.260	1040
7/01	23.7	6.3	-90	540	405	800	700	2010	32	95	4620	9180	0.090	1120
8/01	23.3	6.5	-80	540	408	830	730	2020	21	85	4610	9220	0.060	1100
9/01	22.9	6.3	-60	550	404	820	680	2040	20	84	4430	9000	0.640	1060
10/01	22.9	6.3	-60	550	398	810	640	2050	6.0	83	4410	8940	n.m.	n.m.
11/01	22.9	6.2	-40	530	383	860	470	1860	<0.1	93	4170	8370	n.m.	n.m.
12/01	23.1	6.1	-80	550	415	810	650	2010	<0.1	97	4440	8970	n.m.	n.m.
01/02	22.7	6.3	-60	530	400	820	650	1970	<0.1	98	4490	8960	0.052	910
02/02	22.6	6.0	-50	550	392	810	620	1890	<0.1	103	4580	8930	0.143	910
03/02	22.8	6.1	n.m.	560	396	800	580	1950	<0.1	94	4590	8970	0.099	1180
04/02	23.2	6.4	-30	550	394	810	680	2000	11.8	92	4420	8940	0.061	700
05/02	23.3	6.4	-150	560	394	800	640	1910	<0.1	91	4830	9220	0.047	650
06/02	23.4	6.5	-100	580	419	800	720	2010	<0.1	85	4660	9270	0.069	670
07/02	23.4	6.5	-150	530	395	750	700	1950	24	83	4710	9110	0.051	670
08/02	23.8	6.7	-110	540	392	780	610	1950	<0.1	83	4690	9030	0.059	690
09/02	23.5	6.4	-130	540	396	780	620	1940	<0.1	89	4520	8880	0.170	770
10/02	23.3	6.4	-150	550	411	770	570	1930	22	88	4440	8760	0.164	810
12/02	20.8	6.4	-70	540	388	790	530	1810	<0.1	93	4380	8530	0.290	670
01/03	20.8	6.1	-70	550	392	760	530	1840	10	92	4440	8600	0.310	680

Table A3 (continues on next page).

Site 14														
Date (mo/yr)	T (°C)	pH	Eh (mV)	Na^+ (mg/l)	K^+ (mg/l)	Mg^{2+} (mg/l)	Ca^{2+} (mg/l)	Cl^- (mg/l)	NO_3^- (mg/l)	SO_4^{2-} (mg/l)	HCO_3^- (mg/l)	TDS (mg/l)	CH_4 cc/l STP	CO_2 cc/l STP
03/03	n.m.	n.m.	n.m.	540	402	730	590	1950	12	92	4270	8580	0.391	790
04/03	23.4	6.5	-180	590	403	790	680	2160	117	95	4270	8980	0.046	810
06/03	23.5	n.m.	-220	560	431	780	720	1880	<0.1	88	4740	9200	0.165	620
07/03	23.1	6.3	-150	540	408	770	680	1950	<0.1	95	4710	9150	n.m.	n.m.
08/03	23.7	6.4	-200	550	421	830	670	1950	<0.1	99	4590	9120	0.117	790
09/03	22.8	6.5	-110	550	422	790	690	2060	<0.1	91	4620	9220	0.117	770
10/03	21.9	6.5	-110	540	417	810	630	1930	22.3	121	4670	9120	0.6177	830
12/03	22.6	6.4	-140	550	418	760	670	1930	<0.1	108	4660	9100	0.160	760
01/04	22.2	6.3	-180	530	405	760	670	1930	<0.1	101	4560	8950	n.m.	n.m.
03/04	22.2	6.3	-150	530	413	730	670	1850	<0.1	124	4610	8930	0.671	710
04/04	21.4	6.3	-170	510	405	740	670	1960	<0.1	110	4510	8910	0.089	890
05/04	22.5	6.5	-160	530	405	790	720	1930	<0.1	113	4690	9190	0.092	680
06/04	23.0	6.7	-120	540	413	780	690	1870	<0.1	112	4740	9130	n.m.	n.m.
09/04	22.8	6.6	-140	560	428	780	620	2050	<0.1	101	4450	8980	0.050	750
10/04	22.4	6.4	-150	560	427	830	570	1970	<0.1	112	4340	8810	0.207	760
11/04	22.2	6.3	-110	530	409	750	550	1940	<0.1	96	4270	8540	0.235	620
12/04	22.0	6.4	-110	530	407	780	550	1940	<0.1	88	4290	8590	0.066	650
01/05	22.0	n.m.	-80	530	410	780	590	1890	<0.1	115	4270	8580	n.m.	n.m.
03/05	22.4	6.2	-140	530	408	780	490	1830	<0.1	106	4270	8400	0.481	740
04/05	22.3	6.2	2.0	520	398	750	580	1850	<0.1	93	4320	8500	0.208	610
05/05	22.3	6.2	-140	510	397	740	550	1850	<0.1	89	4210	8340	n.m.	n.m.
06/05	22.6	6.4	-130	550	404	790	640	1980	<0.1	89	4460	8920	0.097	520
07/05	22.7	6.5	-140	510	387	720	620	1980	<0.1	89	4150	8460	0.137	590
08/05	22.6	n.m.	n.m.	540	416	780	660	1990	<0.1	87	4420	8900	0.430	840
10/05	22.7	n.m.	n.m.	550	418	780	570	2060	<0.1	95	4160	8620	n.m.	n.m.
11/05	21.4	6.3	n.m.	540	414	780	590	1940	<0.1	94	4270	8630	0.430	700
12/05	22.3	6.2	n.m.	570	422	810	590	2060	<0.1	85	4270	8810	0.184	720
01/06	21.8	6.3	n.m.	520	380	730	540	1910	<0.1	99	3990	8170	0.286	740
03/06	22.3	6.4	n.m.	540	397	760	550	2000	<0.1	106	4060	8400	n.m.	n.m.
10/06	22.8	6.4	-80	540	412	790	590	1890	<0.1	89	4460	8770	0.143	770
02/07	22.0	n.m.	n.m.	540	407	780	570	1990	<0.1	84	4280	8660	n.m.	n.m.
06/07	22.5	6.0	-200	550	410	780	670	1960	<0.1	91	4470	8930	0.307	800

Table A3 (continued from previous page).

Site 19												
Date (mo/yr)	T (°C)	pH	Eh (mV)	Na^+ (mg/l)	K^+ (mg/l)	Mg^{2+} (mg/l)	Ca^{2+} (mg/l)	Cl^- (mg/l)	NO_3^- (mg/l)	SO_4^{2-} (mg/l)	HCO_3^- (mg/l)	TDS (mg/l)
11/98	21.0	6.6	140	195	361	119	136	331	74	196	1210	2500
1/99	20.9	6.6	130	212	386	130	110	326	84	210	1130	2460
3/99	16.9	7.1	170	202	354	114	93	307	72	183	1090	2300
5/99	21.1	6.7	90	193	360	106	97	266	78	189	1020	2200
10/99	20.8	6.7	180	207	368	122	99	294	112	195	1150	2440
11/99	20.7	6.6	230	203	384	128	110	299	107	191	1140	2390
3/00	20.0	6.6	110	219	381	121	97	283	77	191	1170	2440
5/00	20.9	6.7	140	217	380	118	93	284	73	184	1170	2410
7/00	21.3	6.7	200	206	364	129	107	296	74	191	1230	2470
10/00	20.8	6.7	160	216	385	132	92	300	76	191	1240	2510
11/00	20.7	6.5	180	214	371	132	97	328	79	208	1280	2590
1/01	19.2	6.8	n.m.	203	414	131	120	323	71	191	1240	2570
3/01	20.0	6.5	n.m.	218	371	130	112	310	76	201	1230	2560
4/01	20.8	6.5	150	215	375	129	91	300	72	182	1230	2490
5/01	21.2	6.6	150	204	362	129	110	314	98	193	1250	2520
6/01	21.0	6.5	260	220	377	137	111	327	73	199	1250	2560
7/01	21.4	6.5	210	228	396	140	103	331	80	201	1260	2600
8/01	22.5	6.6	190	225	389	133	107	320	54	195	1290	2580
9/01	20.9	6.5	230	232	396	142	122	341	60	205	1270	2630
10/01	20.9	6.5	180	242	404	148	122	341	72	191	1280	2650
11/01	20.3	6.6	190	226	397	142	114	339	77	216	1310	2680
12/01	20.2	6.6	110	221	379	130	104	322	65	207	1280	2580
01/02	20.6	6.3	140	216	379	135	111	338	77	222	1290	2630
02/02	20.1	6.5	240	229	385	128	102	308	70	192	1240	2520
03/02	20.0	6.1	n.m.	226	396	131	107	334	61	217	1230	2570
04/02	20.4	6.5	-60	227	395	130	105	330	47	213	1250	2560
05/02	21.0	6.6	150	222	379	133	100	319	73	195	1270	2550
06/02	21.3	6.6	170	231	389	131	102	320	76	194	1250	2560
07/02	21.5	6.5	150	237	400	134	106	327	75	196	1270	2610
08/02	21.1	6.6	160	235	394	130	98	329	76	206	1270	2610
09/02	20.4	6.6	110	232	391	131	98	334	74	206	1310	2640
10/02	20.8	6.5	140	235	390	128	96	317	69	195	1320	2620
12/02	20.9	6.5	n.m.	231	365	131	117	320	72	204	1310	2620
12/02	19.8	6.5	120	227	393	130	92	291	62	181	1280	2530
01/03	19.2	6.2	120	224	375	125	93	300	71	199	1260	2520
03/03	n.m.	n.m.	n.m.	211	335	103	93	239	122	210	1030	2240
04/03	20.8	6.7	150	192	310	101	99	245	136	222	920	2120
05/03	20.8	6.5	160	164	301	87	86	189	131	193	870	1940

Table A4 (continues on next page).

Site 19												
Date (mo/yr)	T (°C)	pH	Eh (mV)	Na^+ (mg/l)	K^+ (mg/l)	Mg^{2+} (mg/l)	Ca^{2+} (mg/l)	Cl^- (mg/l)	NO_3^- (mg/l)	SO_4^{2-} (mg/l)	HCO_3^- (mg/l)	TDS (mg/l)
06/03	20.9	n.m.	160	160	287	86	94	186	136	190	850	1910
07/03	21.4	6.6	160	153	278	85	103	197	128	192	850	1900
09/03	21	6.5	n.m.	179	326	107	111	261	104	206	1040	2230
10/03	20.3	6.6	130	190	333	118	112	246	85	179	1130	2280
11/03	18.4	6.5	180	198	351	115	119	280	93	202	1160	2400
12/03	18.4	6.5	120	200	360	110	113	268	85	190	1150	2370
01/04	18.5	6.3	110	193	350	109	110	270	82	190	1140	2340
02/04	n.m.	6.8	140	192	346	111	110	268	75	189	1150	2330
03/04	19.8	6.8	140	205	363	116	112	285	68	190	1160	2380
04/04	17.6	6.6	120	210	369	118	107	296	68	198	1200	2405
05/04	17.6	6.6	50	211	373	122	108	292	73	196	1200	2450
06/04	21.8	6.5	90	213	388	124	62	300	66	196	1190	2410
08/04	n.m.	n.m.	n.m.	219	390	130	107	317	71	205	1230	2540
09/04	21.6	6.6	10	224	401	130	108	326	80	212	1260	2610
10/04	21.3	6.5	90	229	407	139	108	322	76	208	1270	2620
11/04	19.6	6.4	120	226	400	130	108	326	78	206	1300	2640
12/04	19.6	6.5	120	226	403	134	107	327	78	207	1300	2650
01/05	19.3	n.m.	70	224	403	130	101	308	78	199	1270	2580
03/05	19.4	6.4	90	223	404	134	89	300	74	195	1260	2540
04/05	19.8	6.4	120	224	397	130	108	309	76	196	1260	2570
05/05	20.9	6.4	100	216	385	128	104	296	74	191	1260	2530
06/05	21.6	6.4	140	222	399	132	108	326	76	204	1260	2590
07/05	21.9	6.6	200	224	401	134	111	326	71	204	1260	2600
08/05	22.5	n.m.	n.m.	222	397	134	117	339	81	212	1260	2630
10/05	20.8	n.m.	n.m.	227	404	137	113	338	81	215	1270	2650
11/05	20.1	6.4	n.m.	231	413	140	112	339	80	213	1280	2660
12/05	18.2	6.5	n.m.	237	404	141	113	353	79	212	1260	2660
03/06	19.4	6.5	n.m.	230	390	136	107	336	79	204	1260	2610
06/06	21.2	6.3	n.m.	244	433	150	123	389	100	246	1260	2790
10/06	20.8	6.5	100	240	420	150	121	369	89	230	1340	2810
02/07	19.1	n.m.	n.m.	236	410	143	114	339	82	211	1320	2720
06/07	21.8	6.5	100	212	363	125	108	304	62	197	1160	2410
02/08	19.7	6.8	130	213	371	123	105	298	68	197	1170	2420
05/08	20.3	6.9	120	205	355	117	99	270	57	185	1150	2320
10/08	20.7	7.0	120	203	348	113	97	277	70	183	1140	2310
04/10	19.2	6.6	200	167	290	104	93	229	68	168	980	2000
07/10	21.5	6.6	n.m.	182	326	100	83	234	69	170	1040	2100
07/11	22.3	7.0	210	194	340	109	89	256	80	184	1080	2220

Table A4 (continued from previous page).

Site 29														
Date (mo/yr)	T (°C)	pH	Eh (mV)	Na^+ (mg/l)	K^+ (mg/l)	Mg^{2+} (mg/l)	Ca^{2+} (mg/l)	Cl^- (mg/l)	NO_3^- (mg/l)	SO_4^{2-} (mg/l)	HCO_3^- (mg/l)	TDS (mg/l)	CH_4 cc/l STP	CO_2 cc/l STP
5/98	21.7	7.0	-30	163	225	68	73	153	4.4	241	732	1660	2.2E-2	56
11/98	21.5	7.1	-604	158	229	65	68	180	2.2	248	738	1690	2.8E-2	57
1/99	21.4	7.3	-15	162	234	73	79	191	2.5	272	750	1760	4.8E-2	44
5/99	21.5	7.4	-40	151	213	69	58	148	1.4	230	628	1500	2.0E-1	41
10/99	20.9	7.0	120	162	217	63	82	149	3.7	226	1007	1910	6.9E-2	43
11/99	21.8	6.8	120	150	217	74	77	163	2.9	235	683	1700	2.7E-2	60
3/00	19.7	7.1	110	160	220	67	75	154	8.5	232	702	1610	4.1E-2	44
5/00	21.2	7.5	70	166	231	68	68	161	6.2	239	720	1570	n.m.	n.m.
7/00	21.4	7.2	55	151	211	70	83	164	7.5	234	732	1660	n.m.	n.m.
10/00	21.2	7.1	70	168	219	68	68	146	4.1	228	720	1610	2.2E-2	67
11/00	21.3	6.9	100	156	232	70	72	165	3.8	247	744	1670	4.2E-2	54
1/01	20.3	6.9	n.m.	155	227	65	71	166	3.1	237	723	1730	3.8E-2	83
3/01	21.3	6.9	n.m.	166	226	74	83	176	3.8	251	781	1770	n.m.	78
4/01	21.4	6.8	70	161	229	80	80	158	3.8	227	787	1710	6.3E-2	127
5/01	21.5	7.0	90	152	213	74	79	169	2.9	250	738	1680	6.4E-2	76
6/01	21.5	6.9	100	160	218	74	72	169	5.5	247	702	1650	n.m.	n.m.
7/01	21.5	6.7	150	162	223	70	73	165	9.2	241	720	1660	n.m.	n.m.
8/01	22.0	6.8	70	159	222	72	73	156	0.6	230	726	1640	n.m.	n.m.
9/01	21.5	6.9	200	166	223	75	78	172	4.3	245	741	1700	n.m.	n.m.
10/01	21.6	7.0	110	149	217	67	70	163	10.4	236	738	1650	9.6E-3	70
01/02	21.8	6.7	90	153	211	66	74	176	<0.1	262	717	1660	n.m.	n.m.
02/02	20.6	6.7	110	159	214	65	72	148	7	229	683	1580	5.4E-2	61
03/02	21.1	6.7	n.m.	157	232	70	69	182	<0.1	259	711	1680	2.3E-2	62
04/02	21.5	6.8	70	163	229	70	81	183	<0.1	257	747	1730	3.4E-2	165
05/02	21.9	6.9	110	159	211	67	65	164	<0.1	236	726	1630	n.m.	n.m.
06/02	21.8	6.9	60	162	225	68	77	174	<0.1	236	723	1670	4.9E-2	69
07/02	21.5	6.9	-5	164	224	66	74	154	<0.1	230	717	1630	8.7E-2	62
09/02	21.4	6.9	-25	154	211	60	67	159	<0.1	234	705	1590	1.4E-1	59
09/02	21.1	7.3	-50	151	209	60	66	155	<0.1	231	702	1570	7.1E-2	45
10/02	21.2	7.0	-30	163	220	65	67	159	<0.1	239	708	1620	1.4E-1	62
12/02	21.0	7.0	40	155	215	63	66	138	<0.1	221	781	1640	1.2E-1	52
12/02	20.9	6.9	50	158	218	64	69	142	<0.1	220	732	1600	8.6E-2	60
01/03	21.7	6.8	20	166	215	65	71	156	3	247	723	1650	1.2E-1	61
03/03	21.3	7.2	80	175	213	64	63	163	<0.1	250	686	1620	8.5E-2	58
04/03	21.6	6.9	-90	170	211	64	69	181	1	269	672	1640	6.7E-2	56
05/03	21.5	n.m.	70	153	216	63	69	157	1	249	653	1560	6.0E-2	63
07/03	21.8	7.0	60	152	214	61	68	153	<0.1	243	641	1530	n.m.	n.m.

Table A5 (continues on next page).

Site 29														
Date (mo/yr)	T (°C)	pH	Eh (mV)	Na^+ (mg/l)	K^+ (mg/l)	Mg^{2+} (mg/l)	Ca^{2+} (mg/l)	Cl^- (mg/l)	NO_3^- (mg/l)	SO_4^{2-} (mg/l)	HCO_3^- (mg/l)	TDS (mg/l)	CH_4 cc/l STP	CO_2 cc/l STP
08/03	21.8	7.0	80	142	204	62	72	142	0	235	653	1510	3.3E-2	56
09/03	21.3	6.8	n.m.	140	207	63	69	133	3	239	628	1480	1.9E-2	66
10/03	20.9	7.0	130	142	207	60	64	123	<0.1	211	647	1450	1.9E-2	63
11/03	21.4	7.0	60	148	215	60	67	140	3	241	637	1510	8.6E-3	58
12/03	21.1	7.0	30	146	213	59	69	134	<0.1	231	671	1520	<0.001	54
01/04	20.7	6.7	50	136	205	59	69	131	4	231	634	1470	n.m.	n.m.
03/04	21.0	6.2	-30	143	207	59	69	123	4	242	637	1490	2.9E-2	59
04/04	20.8	7.0	30	144	209	59	69	146	2	247	653	1530	2.9E-2	60
05/04	21.1	7.0	40	143	204	63	75	144	0	239	647	1510	2.9E-2	59
06/04	21.3	n.m.	10	143	211	60	68	135	0	230	647	1490	1.2E-2	55
09/04	20.9	7.0	40	143	211	60	71	148	0	257	641	1530	<0.001	23
10/04	20.7	7.1	30	130	206	50	68	108	0	239	637	1440	3.3E-1	33
11/04	20.3	6.9	70	139	206	57	67	139	4	238	637	1490	<0.001	29
12/04	20.1	7.3	30	140	207	60	69	138	2	245	631	1490	6.6E-1	10
03/05	20.3	6.9	70	140	211	60	63	132	0	236	607	1450	3.8E-3	39
04/05	19.5	7.3	30	139	214	60	73	145	0	240	607	1480	<0.001	17
05/05	20.8	6.8	-2	136	204	59	70	133	<0.1	234	604	1440	n.m.	n.m.
06/05	21.1	7.3	80	143	213	58	66	136	<0.1	240	607	1460	2.9E-3	23
07/05	21.1	6.7	90	134	201	58	70	136	<0.1	241	580	1420	3.9E-3	14
08/05	20.5	n.m.	n.m.	135	203	58	69	135	<0.1	241	580	1420	4.9E-3	10
10/05	20.4	n.m.	n.m.	135	203	58	69	135	<0.1	241	580	1420	n.m.	n.m.
11/05	18.1	6.9	n.m.	132	200	58	69	128	<0.1	237	592	1420	9.3E-3	30
12/05	19.6	7.6	n.m.	139	204	60	71	140	<0.1	254	576	1440	3.6E-3	10
01/06	19.7	7.6	n.m.	131	195	59	73	131	<0.1	244	576	1410	2.8E-3	12
03/06	19.5	7.4	n.m.	134	195	56	67	133	<0.1	243	576	1410	<0.001	20
06/06	20.2	7.0	n.m.	135	206	61	74	135	<0.1	252	598	1460	5.5E-3	18
10/06	19.7	6.9	150	n.m.	n.m.	n.m.	n.m.	n.m.	n.m.	n.m.	n.m.	n.m.	2.3E-2	42
02/07	19.6	n.m.	n.m.	135	200	58	72	136	<0.1	248	570	1420	2.8E-3	25
06/07	20.4	7.6	30	132	198	59	76	155	<0.1	233	570	1420	3.3E-3	14
02/08	19.6	7.6	-10	128	193	58	75	161	<0.1	228	564	1410	4.2E-3	16
05/08	19.7	7.6	100	124	187	52	69	124	<0.1	228	525	1310	2.8E-3	10
10/08	19.5	7.4	70	120	181	50	64	120	<0.1	220	512	1270	4.0E-3	12
07/09	19.8	7.4	80	112	177	48	62	112	<0.1	204	506	1220	n.m.	n.m.
04/10	19.7	7.4	150	106	166	45	54	112	<0.1	197	467	1150	5.9E-3	16
07/10	22.2	7.1		107	173	43	55	113	<0.1	192	458	1140	7.8E-3	24
07/11	19.3	7.1	140	108	170	41	51	111	<0.1	180	451	1110	4.0E-3	20

Table A5 (continued from previous page).

Site 31														
Date (mo/yr)	T (°C)	pH	Eh (mV)	Na^+ (mg/l)	K^+ (mg/l)	Mg^{2+} (mg/l)	Ca^{2+} (mg/l)	Cl^- (mg/l)	NO_3^- (mg/l)	SO_4^{2-} (mg/l)	HCO_3^- (mg/l)	TDS (mg/l)	CH_4 cc/l STP	CO_2 cc/l STP
5/98	19.0	7.0	-90	309	285	191	141	383	5.8	173	1650	3140	0.0001	130
11/98	19.1	7.0	-90	313	281	187	133	411	2.7	167	1630	3120	0.0001	170
1/99	18.4	6.9	-90	300	269	178	124	448	0.0	183	1590	3100	0.3000	140
3/99	20.1	7.0	-100	310	282	183	141	456	1.2	178	1590	3140	0.0050	80
5/99	20.2	7.0	-120	285	270	168	134	395	0.2	185	1380	2830	0.0004	130
10/99	19.7	7.2	-110	303	277	175	128	412	0.3	177	1680	3150	0.0030	120
11/99	20.7	6.8	-90	297	275	184	154	378	0.2	164	1560	3070	0.0400	230
3/00	20.5	7.0	-90	302	277	172	135	391	8.7	177	1620	3150	n.m.	n.m.
5/00	20.4	6.9	-80	318	289	182	141	403	1.2	176	1650	3140	<0.0001	170
7/00	19.8	6.8	-90	290	270	186	139	382	3.2	173	1540	2980	<0.0001	120
10/00	18.8	6.7	-110	301	286	190	122	383	<0.1	176	1650	3110	<0.0001	170
11/00	20.0	6.8	-90	300	262	187	137	384	<0.1	178	1700	3150	n.m.	n.m.
1/01	19.7	6.9	n.m.	288	256	177	132	383	<0.1	165	1630	3060	n.m.	n.m.
3/01	19.6	6.8	n.m.	306	271	192	159	415	<0.1	185	1650	3150	<0.0001	200
4/01	20.6	7.0	-90	298	263	187	127	414	2.0	169	1710	3210	0.05	180
5/01	20.4	6.8	-50	281	266	189	134	412	0.8	208	1580	3070	<0.0001	180
6/01	20.3	6.8	-10	291	278	199	151	423	1.8	211	1580	3140	n.m.	n.m.
7/01	20.5	6.7	-110	309	280	200	159	432	6.7	200	1690	3280	n.m.	n.m.
8/01	20.7	6.9	-70	287	286	200	130	381	7.3	240	1640	3170	<0.0001	120
9/01	19.9	6.8	-50	304	271	185	148	385	4.3	175	1680	3150	<0.0001	120
10/01	19.8	6.8	-40	282	291	194	148	408	4.3	234	1520	3080	<0.0001	130
11/01	19.9	6.7	-60	315	281	201	141	416	<0.1	221	1690	3260	<0.0001	150
12/01	20.0	6.9	-70	292	259	181	139	387	<0.1	186	1660	3100	n.m.	n.m.
1/02	20.3	6.7	-70	285	263	179	140	373	<0.1	174	1680	3090	0.01	140
2/02	19.9	6.8	-30	320	281	195	138	407	<0.1	190	1680	3210	<0.0001	130
3/02	20.1	6.8		305	269	188	138	418	<0.1	199	1680	3200	0.1	200
4/02	20.0	6.9	-80	294	277	187	145	374	<0.1	194	1650	3120	0.1	210
5/02	20.1	6.9	-60	298	273	195	136	406	<0.1	204	1710	3220	<0.0001	160
6/02	20.1	6.8	-30	n.m.	n.m.	n.m.	n.m.	n.m.	n.m.	n.m.	n.m.	n.m.	0.01	120

Table A6 (continues on next page).

Site 31														
Date (mo/yr)	T (°C)	pH	Eh (mV)	Na^+ (mg/l)	K^+ (mg/l)	Mg^{2+} (mg/l)	Ca^{2+} (mg/l)	Cl^- (mg/l)	NO_3^- (mg/l)	SO_4^{2-} (mg/l)	HCO_3^- (mg/l)	TDS (mg/l)	CH_4 cc/l STP	CO_2 cc/l STP
7/02	19.9	6.9	-80	n.m.	n.m.	n.m.	n.m.	n.m.	n.m.	n.m.	n.m.	n.m.	0.3	130
8/02	19.9	6.9	-80	n.m.	n.m.	n.m.	n.m.	n.m.	n.m.	n.m.	1700	n.m.	0.4	130
9/02	19.5	7.0	-80	315	264	179	121	370	<0.1	166	1690	3100	0.5	140
10/02	19.8	6.9	-110	305	278	182	153	413	<0.1	182	1690	3210	0.15	170
12/02	19.7	7.0	-90	311	267	185	125	338	<0.1	149	1720	3100	0.5	150
12/02	19.6	7.0	-110	306	266	181	120	355	<0.1	159	1750	3140	0.3	110
1/03	19.0	6.8	-87	305	256	174	118	350	<0.1	160	1760	3130	0.4	140
2/03	n.m.	n.m.	n.m.	n.m.	n.m.	n.m.	n.m.	n.m.	n.m.	n.m.	n.m.	n.m.	0.4	130
3/03	19.4	7.0	-40	325	213	177	120	359	<0.1	198	1640	3040	0.2	140
4/03	19.8	6.8	-90	296	275	186	129	398	3	215	1670	3170	0.2	130
5/03	19.6	n.m.	-100	286	285	178	105	390	<0.1	198	1700	3140	0.0003	110
6/03	20.3	n.m.	-90	283	291	176	117	390	<0.1	206	1700	3160	<0.0001	130
7/03	n.m.	n.m.	n.m.	302	294	195	121	368	<0.1	195	1650	3120	n.m.	n.m.
8/03	n.m.	n.m.	n.m.	264	271	177	103	308	<0.1	190	1620	2930	n.m.	n.m.
9/03	n.m.	n.m.	n.m.	265	267	191	110	358	2	173	1574	2940	0.5	130
10/03	n.m.	n.m.	n.m.	306	277	189	115	332	<0.1	141	1690	3050	n.m.	n.m.
11/03	n.m.	n.m.	n.m.	309	276	182	140	389	<0.1	171	1710	3180	0.4	130
12/03	n.m.	n.m.	n.m.	311	286	172	125	367	<0.1	163	1690	3120	0.7	150
1/04	18.6	7.10	-170	296	272	168	122	345	<0.1	154	1650	3010	0.6	150
2/04	n.m.	n.m.	n.m.	n.m.	n.m.	n.m.	n.m.	n.m.	n.m.	n.m.	n.m.	n.m.	0.5	150
3/04	19.5	7.20	-130	298	279	180	129	355	<0.1	177	1660	3080	0.4	150
4/04	19.6	6.80	7	294	269	173	125	366	9	163	1600	3000	0.8	140
5/04	19.4	6.9	-150	296	269	172	119	417	<0.1	24	1620	2910	0.6	160
6/04	19.9	n.m.	-110	293	272	175	119	325	<0.1	143	1680	3000	<0.0001	150
8/04	n.m.	n.m.	n.m.	290	266	171	119	356	<0.1	158	1600	2960	0.5	120
9/04	19.1	7.0	-180	295	273	172	115	356	<0.1	160	1660	3030	0.6	130
10/04	19	6.9	-100	299	269	189	114	365	<0.1	166	1640	3040	0.6	140
11/04	19.1	6.9	-100	299	272	174	123	353	<0.1	167	1690	3070	0.5	150
1/05	19.1	n.m.	-130	299	278	179	116	353	<0.1	158	1650	3030	0.6	140

Table A6 (continued from previous page).

Olivella													
Date (mo/yr)	T (°C)	pH	Eh (mV)	Na^+ (mg/l)	K^+ (mg/l)	Mg^{2+} (mg/l)	Ca^{2+} (mg/l)	Cl^- (mg/l)	NO_3^- (mg/l)	SO_4^{2-} (mg/l)	HCO_3^- (mg/l)	TDS (mg/l)	CO_2 cc/l STP
5/98	13.2	8.0	110	50	72	22	78	36	56	52	400	730	n.m.
11/98	14.1	7.7	180	52	75	20	70	37	60	57	400	740	8
1/99	10.7	8.3	60	52	74	23	65	38	61	60	350	690	7
3/99	9.2	8.2	190	52	75	22	63	37	60	63	320	660	4
5/99	12.8	8.0	120	53	73	24	79	38	58	60	340	690	7
10/99	13.7	6.8	-150	55	78	24	81	38	64	64	410	770	19
11/99	12.7	8.1	240	51	80	27	68	38	64	62	370	720	3
3/00	10.8	8.2	230	54	70	21	60	44	52	57	310	620	4
5/00	12.7	7.9	130	53	76	22	78	37	57	60	320	640	3
7/00	13.4	7.9	210	51	73	25	76	36	60	62	430	770	7
10/00	13.5	7.7	160	56	78	25	72	34	56	61	410	760	7
11/00	13.3	7.8	170	50	72	22	66	36	51	60	390	700	9
1/01	9.3	8.3	n.m.	52	60	20	61	32	42	48	350	670	2
3/01	12.2	8.1	n.m.	50	72	24	71	34	51	50	370	680	3
4/01	12.4	8.0	150	47	69	23	69	32	40	46	400	690	8
5/01	13.2	7.9	180	47	69	22	67	34	42	53	400	700	7
6/01	13.5	8.0	280	49	72	22	74	41	44	59	410	730	n.m.
7/01	13.7	8.0	140	54	76	23	75	37	46	53	430	750	n.m.
8/01	13.8	7.8	240	53	76	24	75	37	45	53	430	750	n.m.
9/01	13.6	7.9	230	55	76	25	74	36	49	53	430	770	5
10/01	13.8	7.8	330	55	75	24	67	33	45	51	410	730	4
11/01	11.4	8.0	430	54	73	22	68	36	45	53	380	700	5
12/01	7.2	7.9	250	54	68	20	68	42	47	60	370	680	n.m.
01/02	8.4	7.9	290	51	68	21	69	40	49	60	370	690	4
02/02	9.7	8.2	190	52	69	20	64	41	43	57	380	690	n.m.
03/02	9.1	8.1	160	51	71	22	66	36	38	54	360	660	3
04/02	10.7	8.0	110	53	70	23	66	37	36	54	380	680	n.m.
05/02	13.2	8.0	140	54	71	23	64	39	42	57	380	700	5
06/02	13.2	7.9	170	56	76	23	74	44	43	56	380	710	4
07/02	13.6	7.8	160	57	76	23	73	43	43	61	380	720	4
08/02	13.9	7.9	180	54	75	22	69	43	46	62	390	720	6
09/02	12.5	7.9	130	52	72	21	63	41	38	59	380	680	n.m.
10/02	13.6	7.8	180	51	71	22	69	40	38	55	390	700	3
12/02	11.6	8.3	110	57	67	21	65	35	38	52	370	670	5
12/02	8.3	8.2	30	49	67	19	59	35	34	52	350	630	n.m.
01/03	9.7	8.1	170	51	67	20	62	40	35	55	360	650	4
03/03	13.2	7.9	180	58	73	21	58	39	58	60	430	760	9
04/03	13.0	7.6	250	57	73	22	84	49	49	73	390	750	4
05/03	13.3	n.m.	210	55	74	22	87	39	45	59	440	780	4

Table A7 (continues on next page).

Olivella													
Date (mo/yr)	T (°C)	pH	Eh (mV)	Na^+ (mg/l)	K^+ (mg/l)	Mg^{2+} (mg/l)	Ca^{2+} (mg/l)	Cl^- (mg/l)	NO_3^- (mg/l)	SO_4^{2-} (mg/l)	HCO_3^- (mg/l)	TDS (mg/l)	CO_2 cc/l STP
06/03	13.7	n.m.	190	55	76	23	88	39	43	58	450	790	12
07/03	14.7	7.9	170	55	77	22	83	41	45	62	420	770	n.m.
08/03	14.3	7.6	100	52	73	23	99	38	49	58	460	810	6
09/03	14.0	7.7	-50	53	76	23	89	39	44	61	440	790	5
10/03	13.8	7.8	170	51	73	22	82	36	42	51	420	740	5
11/03	13.4	7.9	210	52	73	22	75	36	41	52	420	740	6
12/03	11.2	7.8	90	53	71	23	78	35	40	48	420	740	6
01/04	8.80	7.9	200	49	69	23	77	37	37	46	420	720	n.m.
02/04	7.90	7.8	190	47	66	22	74	35	31	45	390	680	4
03/04	8.6	7.9	140	54	69	22	72	35	33	45	420	710	3
4/04	11.9	7.7	150	47	67	21	72	34	29	45	400	680	4
5/04	12.8	7.9	80	50	71	22	79	36	40	52	410	720	7
06/04	13.4	n.m.	110	49	72	22	85	36	37	55	420	740	5
08/04	n.m.	n.m.	n.m.	50	70	23	76	35	33	54	420	730	5
09/04	13.7	7.6	70	54	76	23	89	44	48	71	430	790	6
10/04	13.8	7.7	70	55	79	26	94	39	37	62	470	830	6
11/04	12.9	7.9	20	53	74	24	86	36	37	58	450	790	5
12/04	12.5	7.8	150	49	70	21	67	33	30	51	390	680	5
01/05	12.5	n.m.	40	49	69	22	84	35	38	52	430	740	3
03/05	12.7	n.m.	80	44	66	23	85	29	35	40	430	730	5
04/05	13.0	7.9	80	49	70	23	89	33	34	50	450	760	6
05/05	13.4	7.7	40	51	73	23	92	35	37	54	460	790	n.m.
06/05	13.6	7.7	130	55	76	23	92	37	39	57	460	800	6
07/05	13.8	7.7	220	53	75	23	80	40	37	62	420	750	6
08/05	13.8	n.m.	n.m.	55	77	24	89	40	38	63	440	790	4
09/05	13.7	n.m.	n.m.	54	76	24	89	39	38	61	440	780	n.m.
10/05	13.7	n.m.	n.m.	51	72	22	80	37	31	56	410	720	6
12/05	12.0	7.8	n.m.	51	71	21	69	30	24	44	420	700	2
06/06	13.4	7.6	n.m.	51	73	24	94	35	33	57	460	790	7
10/06	13.8	7.8	240	51	73	24	94	35	33	56	460	790	7
02/07	11.1	n.m.	n.m.	52	72	23	78	38	31	60	420	730	3
06/07	13.3	7.7	200	52	73	24	79	36	32	64	420	750	14
02/08	10.6	8.0	120	52	72	24	82	38	30	64	420	750	3
05/08	12.3	7.5	200	51	70	23	85	32	26	51	420	730	6
10/08	13.4	7.7	20	54	73	24	82	34	35	74	410	750	6
04/10	12.9	8.1	260	45	62	21	81	28	25	56	400	690	5
07/10	13.4	7.8		50	72	22	82	35	30	66	420	740	7
07/11	13.3	7.8	100	54	71	22	81	32	24	64	440	760	8

Table A7 (continued from previous page).